JCI insight

NKp46-expressing human gut-resident intraepithelial Vδ1 T cell subpopulation exhibits high anti-tumor activity against colorectal cancer

Joanna Mikulak, … , Antonino Spinelli, Domenico Mavilio

JCI Insight. 2019. https://doi.org/10.1172/jci.insight.125884.

Research In-Press Preview Gastroenterology Immunology

γδ T cells account for a large fraction of human intestinal intraepithelial lymphocytes (IELs) endowed with potent anti-tumor activities. However, little is known about their origin, phenotype and clinical relevance in colorectal cancer (CRC). To determine γδ IEL gut-specificity, homing and functions, γδ T cells were purified from human healthy blood, lymph nodes, liver, skin, intestine either disease-free or affected by CRC or generated from thymic precursors. The constitutive expression of NKp46 specifically identifies a new subset of cytotoxic Vδ1 T cells representing the largest fraction of gut-resident IELs. The ontogeny and gut-tropism of NKp46^{pos}/Vδ1 IELs depends both on distinctive features of Vδ1 thymic precursors and gut-environmental factors. Either the constitutive presence of NKp46 on tissue-resident Vδ1 intestinal IELs or its induced-expression on IL-2/IL-15 activated Vδ1 thymocytes are associated with anti-tumor functions. Higher frequencies of NKp46^{pos}/Vδ1 IELs in tumor-free specimens from CRC patients correlate with a lower risk of developing metastatic III/IV disease stages. Additionally, our in vitro settings reproducing CRC tumor-microenvironment inhibited the expansion of NKp46^{pos}/Vδ1 cells from activated thymic precursors. These results parallel the very low frequencies of NKp46^{pos}/Vδ1 IELs able to infiltrate CRC, thus providing new insights to either follow-up cancer progression or develop novel adoptive cellular therapies.

Find the latest version:

https://jci.me/125884/pdf

Original Research Article

NKp46-expressing human gut-resident intraepithelial Vδ1 T cell subpopulation exhibits high anti-tumor activity against colorectal cancer

Joanna Mikulak,[1,2] Ferdinando Oriolo,[1,2*] Elena Bruni,[1,2] Alessandra Roberto,[3] Federico S. Colombo,[4] Anna Villa,[5,6] Marita Bosticardo,[5] Ileana Bortolomai,[5] Elena Lo Presti,[7,8] Serena Meraviglia,[7,8] Francesco Dieli,[7,8] Stefania Vetrano,[9,10] Silvio Danese,[9,10] Silvia Della Bella,[1,2] Michele M. Carvello,[11] Matteo Sacchi,[11] Giovanni Cugini,[12] Giovanni Colombo,[12] Marco Klinger[2,13], Paola Spaggiari,[14] Massimo Roncalli,[10-14] Immo Prinz,[15] Sarina Ravens,[15] Biagio di Lorenzo,[16,17] Emanuela Marcenaro,[18-19] Bruno Silva-Santos,[16] Antonino Spinelli,[10,11] and Domenico Mavilio[1,2]*

[1]Unit of Clinical and Experimental Immunology, Humanitas Clinical and Research Center, Rozzano, Milan, Italy.
[2]Department of Medical Biotechnologies and Translational Medicine (BioMeTra), University of Milan, Italy.
[3]Laboratory of Translational Immunology, Humanitas Clinical and Research Center, Rozzano, Milan, Italy.
[4]Humanitas Flow Cytometry Core, Humanitas Clinical and Research Center, Rozzano, Milan, Italy.
[5]San Raffaele Telethon Institute for Gene Therapy (SR-TIGET), Division of Regenerative Medicine, Stem Cells and Gene Therapy, San Raffaele Scientific Institute, Milan, Italy.
[6]Istituto di Ricerca Genetica e Biomedica, Consiglio Nazionale delle Ricerche, Milan, Italy.
[7]Central Laboratory for Advanced Diagnostic and Biomedical Research (CLADIBIOR), University of Palermo, Palermo, Italy.
[8]Department of Biopathology and Medical Biotechnologies (DIBIMED), University of Palermo, Palermo, Italy.
[9]IBD Center, Laboratory of Gastrointestinal Immunopathology, Humanitas Clinical and Research Center, Rozzano, Milan, Italy.
[10]Department of Biomedical Sciences, Humanitas University, Rozzano, Milan, Italy.
[11]Colon and Rectal Surgery Unit, Humanitas Clinical and Research Center, Rozzano, Milan, Italy.
[12]Otorhinolaryngology Department, Humanitas Clinical and Research Center, Rozzano, Milan, Italy
[13]Plastic Surgery Unit, Humanitas Clinical and Research Center, Rozzano, Milan, Italy.
[14] Department of Pathology, Humanitas Clinical and Research Center, Rozzano, Milan, Italy;
[15] Institute of Immunology, Hannover Medical School, Hannover, Germany.
[16]Instituto de Medicina Molecular, Faculdade de Medicina, Universidade de Lisboa, Lisboa, Portugal.
[17]Instituto Superior Técnico, Universidade de Lisboa, Lisbon, Portugal.
[18]Department of Experimental Medicine, University of Genoa, Genoa, Italy.
[19]Centre of Excellence for Biomedical Research, University of Genoa, Genoa, Italy.

**These authors contributed equally to this work*

Corresponding author:
Domenico Mavilio, M.D., Ph.D.
Unit of Clinical and Experimental Immunology
Department of Medical Biotechnologies and Translational Medicine
University of Milan School of Medicine
Humanitas Clinical and Research Center
Via Alessandro Manzoni, 113
Rozzano (Milan), Italy.
Phone: +39-02.8224.5157 - Fax: +39-02.8224.5191
e-mail: domenico.mavilio@unimi.it

Words in Title: ***14***
Words in Abstract: ***200***
Words in the Manuscript: ***11920***
Regular Figures: ***7***
Supplementary Figures: ***7***
Supplementary Table: ***1***
References: ***62***

Abstract

γδ T cells account for a large fraction of human intestinal intraepithelial lymphocytes (IELs) endowed with potent anti-tumor activities. However, little is known about their origin, phenotype and clinical relevance in colorectal cancer (CRC). To determine γδ IEL gut-specificity, homing and functions, γδ T cells were purified from human healthy blood, lymph nodes, liver, skin, intestine either disease-free or affected by CRC or generated from thymic precursors. The constitutive expression of NKp46 specifically identifies a new subset of cytotoxic Vδ1 T cells representing the largest fraction of gut-resident IELs. The ontogeny and gut-tropism of NKp46^{pos}/Vδ1 IELs depends both on distinctive features of Vδ1 thymic precursors and gut-environmental factors. Either the constitutive presence of NKp46 on tissue-resident Vδ1 intestinal IELs or its induced-expression on IL-2/IL-15 activated Vδ1 thymocytes are associated with anti-tumor functions. Higher frequencies of NKp46^{pos}/Vδ1 IELs in tumor-free specimens from CRC patients correlate with a lower risk of developing metastatic III/IV disease stages. Additionally, our *in vitro* settings reproducing CRC tumor-microenvironment inhibited the expansion of NKp46^{pos}/Vδ1 cells from activated thymic precursors. These results parallel the very low frequencies of NKp46^{pos}/Vδ1 IELs able to infiltrate CRC, thus providing new insights to either follow-up cancer progression or develop novel adoptive cellular therapies.

Introduction

The gastrointestinal (GI) tract is considered the largest immunological organ in the human body with both circulating and tissue-specific immune cells either organized in several structures of the lamina propria (LP) or resident within the epithelium. The synergic interactions of immune cells with both epithelial cells and microbiota shape innate and adaptive immune responses, set up the threshold between immune tolerance and effector-functions and also balance the efficacy of checkpoint blockade in cancer immunotherapy (1, 2).

The human gut epithelium is home to large numbers of T cells expressing gamma delta (γδ) T cell receptors (TCR), which account for the main fraction of all intraepithelial lymphocytes (IELs) (3). While the exact functions of γδ IELs remain elusive, they have been suggested to control anti-microbial defense, organ homeostasis and tissue damage repair (4, 5). Indeed, γδ T cell-deficient mice present abnormalities in gut epithelial morphology, reduced MHC class II expression by enterocytes and impaired mucosal IgA production (6, 7). Although γδ T cells originate from common thymic precursors alongside αβ T cells, they are considered innate-like lymphocytes for their rapid and non MHC-restricted effector responses such as cytotoxicity and secretion of type I cytokines (8). Human γδ T cells are broadly divided into two main Vδ1 and Vδ2 subsets based on their TCRδ-chain repertoire (9). Under homeostatic conditions, Vδ2 cells are mainly enriched in peripheral blood where they represent about 5% of all circulating T cells and recognize specifically microbial or stress-/ tumor-induced "phosphoantigens" (8, 10-12). In contrast, Vδ1 cells are preferentially localized in peripheral tissues such as the gut, skin and liver. However, very little is known about their organ-specificity and local antigens/ligands recognition.

Growing evidences confirmed the important role of γδ T lymphocytes in tumor immune-surveillance and provided promising perspectives in cancer immunotherapy (13). Indeed, both Vδ1 and Vδ2 subsets expanded from peripheral blood are endowed with high anti-tumor activities against hematological malignances and solid tumors *in vivo* and *in vitro* (14). Therefore, much effort has been made to improve blood γδ T cell-mediated tumor recognition and killing (15). In this context, we previously showed that the TCR stimulation *in vitro* induces a de novo expression of Natural Cytotoxic Receptors (NCRs) (mainly NKp30) on circulating Vδ1 T cells, thus remarkably increasing their anti-tumor effector functions (16). Hence, NCRs are no longer considered as specific Natural Killer (NK) cell activating receptors (aNKR) and are currently being implemented for developing novel adoptive cellular therapies against cancers (17, 18).

In contrast to the peripheral blood γδ T cells that have received much attention, both phenotype and anti-tumor potentials as well as the mechanisms regulating the homeostasis of human tissue-

resident γδ T cells are still largely unknown. Indeed, while mice share some common innate-like functions of human γδ T cells, they differ significantly in terms of TCR specificity and tissue specialization (19). Nonetheless, several studies reported that in different types of human cancers, including colorectal cancer (CRC), high frequencies of intra-tumoral γδ T cells represent one of most favorable prognostic markers in tumor clinical outcomes (20, 21). Hence, there is a pressing need to better characterize human tissue-resident γδ T lymphocytes in order to understand their impact in the physiopathology of cancer.

The present study identifies a novel subset of gut-resident Vδ1 IELs naturally expressing high levels of NKp46. The presence of this NCR characterizes the largest subset of γδ T cells among intestinal IELs, a population that we could not detect in healthy human skin, lymph nodes, liver and not even in the gut of wild-type mice strains. NKp46^{pos}/Vδ1 IELs share the same phenotypic and anti-tumor effector-functions of NKp46^{pos}/Vδ1 T cells generated from thymic precursors following activation with Interleukin (IL)-2 or IL-15, two cytokines highly enriched in gut microenvironment that confer to Vδ1 thymocytes a specific gut tropism. Low frequencies of NKp46^{pos}/Vδ1 IEL subset in healthy gut specimens of patients affected by CRC are associated with a faster tumor progression and development of metastatic diseases, thus suggesting a protective role and a potential prognostic value of these tissue-resident innate-like lymphocytes in CRC.

Results

Identification of a novel subset of NKp46^{pos} γδ intestinal intraepithelial T lymphocytes.

Human healthy colon specimens obtained from patients who underwent surgical resection for colorectal cancers (CRC) were located at the distal part (≥ 10 cm in length) of the removed tumor core and were considered "tumor-free/healthy" after a conventional macroscopic and microscopic examination by pathologists. Healthy gut specimens were processed to obtain intraepithelial lymphocytes (IELs) and lamina propria lymphocytes (LPLs) (Supplemental Figure 1A-C). As expected (22), the frequency of γδ T cells appeared to be significantly higher among IELs compared to both LPLs and Peripheral Blood Mononuclear Cells (PBMCs) (Figure 1A-B). Unlike circulating γδ T cells, both γδ IELs and LPLs presented high levels of the tissue-resident marker CD69 (23). The different location of intestinal γδ IELs and LPLs was also confirmed by specific high expression on the first subset and not on the second one of CD103, the main adhesion molecule involved in the specific retention of IELs in the epithelial layer (Figure 1C) (24). We also observed that γδ IELs are characterized by a significant higher expression of CD56 and CD8 compared to γδ LPLs, while expressing low surface levels of CD4. These phenotypic features of γδ IELs are also associated with low amounts of inhibitory NKRs (iNKRs) (i.e. NKG2A and KIRs) and high expression of aNKRs (i.e. NKG2C and NKG2D), thus suggesting that γδ IELs are endowed with a high cytolytic potential (Figure 1D).

Circulating γδ T cells do not physiologically express NCRs (16). In contrast, we found that γδ IELs constitutively express high levels of NKp46, while their counterparts from LP showed a significant lower natural expression of this NCR. Although at a minor extent compared to NKp46, γδ IELs are also NKp44^{pos} in contrast to γδ LPLs and PBMCs that have significantly lower surface levels of this NCR. No significant differences were observed for NKp30 surface levels between γδ T intestinal cells (both IELs and LPLs) and PBMCs (Figure 1E, Supplemental Figure 1D). The presence of NKp46^{pos} γδ T cells in the IE compartment of human intestine was also confirmed by confocal microscopy (Supplemental Figure 1E).

CD8^{pos} γδ IELs had been first characterized as a subset of unconventional T cells expressing in their TCR complex the homodimer CD8αα that induces cell hypo-responsiveness/anergy (25). Another study later identified a novel population of high cytotoxic and immune-regulatory intestinal CD8^{pos} γδ T cells carrying the heterodimer CD8αβ. This latter immuno-regulatory subset plays a key role in the homeostasis of Gut-Associated Lymphoid Tissue and in the pathogenesis of inflammatory bowel disease (26). Our results showed that, while the entire population of CD8^{pos} γδ IELs express

significantly higher levels of α rather than β chain, the subset of NKp46^{pos}/CD8^{pos} γδ IELs co-expresses similar levels of α and β chains in their CD8 receptor (Figure 1F).

CD45^{pos}/CD3^{pos} IELs from healthy gut specimens were also analyzed by a dimensionality reduction method that used the t-Distributed Stochastic Neighbor Embedding (t-SNE) algorithm. Two different and separate clusters of NKp46^{neg} (C1) NKp46^{pos} (C2) γδ IELs were identified on the basis of population boundaries distinguishable on the polychromatic flow cytometry density plots (Figure 1G). The related heatmap showed that C1 and C2 are characterized by distinctive phenotypes with higher expression of NKp44, NKp30, CD8β, CD56, NKG2C and NKG2D and lower expression of inhibitory Killer Immunoglobin Receptors (KIRs) in NKp46^{pos} γδ IELs compared to NKp46^{neg} γδ IELs (Figure 1H).

Taken together, this first set of data indicates that the presence of NKp46 identifies a specific cluster of intestinal CD8 γδ IELs carrying the heterodimer CD8αβ and whose phenotype is likely associated with immune effector-functions (i.e. cytotoxicity and cytokine productions) rather than immune-tolerance.

NKp46^{pos} γδ IELs are Vδ1 restricted and preferentially enriched in human intestine.

As expected (25), γδ IELs comprised higher proportions of Vδ1 T cells in contrast to their counterpart in the blood, known to be mainly Vδ2-restricted (8). A consistent fraction of γδ LPLs neither express Vδ1 nor Vδ2 chain, a phenomenon that we also observed within both IEL and PBMC compartments although at a lower extent (Figure 2A). Therefore, the intestinal LP compartment might be, together with human liver, another preferential tissue where other γδ T cell subsets, such as the Vδ3^{pos} one, could reside (27). Interestingly, we found that NKp46 specifically identifies Vδ1 IELs, while Vδ2 IELs express significantly lower amounts of this NCR. NKp44 marks only a small fraction of γδ IELs with the Vδ1 subset expressing significantly higher levels of this NCR compared to the Vδ2 population. Both Vδ1 and Vδ2 IELs express very low levels of NKp30 (Figure 2B-C).

Vδ1 IELs are characterized by a CD4^{neg}/CD8^{pos} phenotype with high surface levels of CD56 and NKG2D while expressing low amounts of NKG2A and KIRs. In contrast, Vδ2 IELs express significantly lower levels of CD8 and CD56 together with significantly higher amounts of NKG2A when compared with their Vδ1 counterpart (Figure 2D). We then purified IELs from matched healthy ileum and colon specimens from patients affected by Crohn's disease and having undergone surgical gut resection. We found similar frequencies of Vδ1 and Vδ2 T IELs both in ileum and colon, with a higher percentage of Vδ1 compared to Vδ2 cells (Supplemental Figure 2A). Again, the NKp46 expression in the ileum is mainly restricted on Vδ1 IELs in both anatomical sites without any

statistically significant differences between ileum and colon (Supplemental Figure 2B). These results indicate that NKp46^{pos}/Vδ1 lymphocytes represent the largest and most ubiquitous γδ T cell population within the IEL compartment of both small and large intestine.

We then determined the constitutive NCR expression on γδ T cells purified from other human healthy tissues known to be highly enriched of these innate-like T cells: skin, liver and lymph nodes (5, 28). Although skin and liver are predominantly enriched with the Vδ1 cell subset over the Vδ2 one, they do not express NCRs in both tissue sites. Similarly, also Vδ1 and Vδ2 T cells purified from lymph nodes are NKp46^{neg} and NKp44^{neg}, while a minor fraction of both subsets is NKp30^{pos} (Supplemental Figure 3).

Even though murine and human γδ T cells differ in several phenotypic features and tissue distribution, Vδ1 T cells have been shown to be more similar between the two species compared to their Vδ2 counterparts (19). Moreover, NKp46 is the only NCR to be phylogenetically conserved in mice and humans (29). Hence, we investigated whether human NKp46^{pos}/Vδ1 IELs have an equivalent in the intestine of BALB/c and C57BL/6 mice strains. Although murine gut contains high frequencies of γδ T IELs, they do not express NKp46. Instead, tissue-resident NK cells from the same murine specimens express, as expected, detectable levels of this NCR and were used as internal positive controls of these experiments in mice (Supplemental Table 1 and Supplemental Figure 4). We also found that the degree of frequency of total γδ IELs and NKp46^{pos}/Vδ1 IELs in the intestine is both age- and sex-independent (Supplemental Figure 5).

Common features but distinct TCR repertoire of NKp46^{pos} and NKp46^{neg} IEL subsets.

The repertoire of γδ TCR was analyzed via high-throughput sequencing of V(D)J-regions of either the γ-chain (TRG) or δ-chain (TRD) expressed on FACS-sorted Vδ1 NKp46^{pos} and NKp46^{neg} IELs. The purity of all sorted samples was ≥ 95% (Supplemental Figure 6). Our data showed that the TRG repertoires of total NKp46^{pos} and NKp46^{neg} Vδ1 IELs is mainly represented by highly expanded Vγ9^{neg} γδ T cell clones (Figure 3A). We also observed more recurrent usage of Vγ4^{pos} sequences in the NKp46^{pos} IEL subset among different individuals (Figure 3B). On the other hand, extended variability of Vγ chains with similar incidence of Vγ9^{pos} and Vγ4^{pos} sequences were presented in NKp46^{neg} IELs. For TRD repertoires, we found a considerable fraction of Vδ2^{pos} sequences within Vδ1 IELs (data not shown), a phenomenon highly similar to what was recently observed in human Vδ1 γδ thymocytes (30). We then focused our analyses only on Vδ1^{pos} IELs and the results showed that the sequences of NKp46^{pos} and NKp46^{neg} γδ subsets are characterized by highly clonal TRD repertoires and the majority of Vδ1 TRD clones uses the Jδ1-joining element (Figure 3C). Notably, the overall TCR

repertoire diversity is largely similar between NKp46^{pos} and NKp46^{neg} IELs (Figure 3D). The number of shared TRG and TRD clones, calculated between all samples, shows only a few overlapping clones within the γδ IEL compartment, mainly Vγ4^{pos} or Vγ9^{pos} (Figure E). Importantly, the most expanded TRG and TRD clones do not overlap between NKp46^{pos} and NKp46^{neg} γδ IELs within the same individual (Figure 3 A, C and E). Taken together, the predominant individual clonal TRD and TDG repertoires of NKp46^{pos} and NKp46^{neg} IEL subsets and the lack of overlapping clones between NKp46^{pos} and NKp46^{neg} γδ IELs suggest that these two IEL subsets emerge from distinct Vδ1 T cell progenitors.

NKp46 expression on γδ IELs is associated with high cytolytic potential and production of IFN-γ.

Cytokines such as IL-10, IL-17, IL-22 and transforming growth factor-β (TGF-β) play an important role in regulating intestinal immune system homeostasis and are highly enriched in the gut mucosa microenvironment (31). In addition, studies have shown that freshly isolated and activated γδ IELs express high levels of lymphotactin/XCL1, a chemokine important for CD8^{pos} T cell activity and chemotaxis (32). Hence, we compared the transcription levels of these cytokines between circulating γδ T cells and fresh FACS-sorted NKp46^{pos} and NKp46^{neg} γδ IELs. Our results showed that both NKp46^{pos} and NKp46^{neg} γδ IELs express similarly high mRNA amounts of IL-22 and lymphotactin/XCL1 compared to blood γδ T cells, thus highlighting their key roles in intraepithelial immune responses and homeostasis. No differences were found for IL-10, IL-17 and TGF-β transcripts between NKp46^{pos} and NKp46^{neg} γδ IELs and circulating γδ T cells (Figure *4*A).

We then analyzed their IFNγ production and cytolytic potential after co-culture with K562 cells, a tumor target widely employed to test innate cell cytotoxicity (33). NKp46^{pos} and γδ IELs showed a significantly increased production of IFNγ in response to the K562 cells compared to their NKp46^{neg} counterparts (Figure 4B). We then observed that the intra-cellular level of Granzyme B (GZMB) is constitutively higher in freshly purified NKp46^{pos} γδ IELs compared to their NKp46^{neg} counterparts. The incubation with K562 cells further increases the amount of newly synthesized intracellularly GZMB both in NKp46^{pos} and NKp46^{neg} γδ IELs. However, the amounts of this cytotoxic granule were significantly higher in the first subset compared to the second one (Figure 4C). We then measured the degree of CD107a expression as a marker of cytolytic activity. Again, the frequencies of CD107a^{pos}/NKp46^{pos} γδ IELs were significantly higher compared to that of CD107^{pos}/NKp46^{neg} γδ IELs following incubation with K562 (Figure 4D). Additional experiments also

confirmed the great cytotoxic potential of NKp46^{pos} γδ IELs in killing human colon adenocarcinoma cell targets cell targets (i.e. SKCO1 and Caco2) (Figure 4E).

To assess the functional relevance of NKp46 in the highly cytotoxic potentials of NKp46^{pos} γδ IELs, we tested the ability of these cells to degranulate either in the presence or in the absence of the specific anti-NKp46 mAb. The results showed that the masking of NKp46 significantly decreases the ability of NKp46^{pos} γδ IELs to kill K562 (Figure 4F), thus demonstrating a direct involvement of this aNKR in tuning the cytotoxicity of this specific epithelial γδ T cell subset.

Human γδ thymocytes resemble the phenotype and functions of NKp46^{pos} Vδ1 IELs following activation.

Maturation of γδ T cells occurs during thymus development that commits γδ T precursors to properly differentiate and migrate to peripheral tissues (34). Recently, it has been also reported that the acquisition of both cytotoxicity and ability to produce IFN-γ by γδ thymic precursors is not associated with the engagement of TCR, but rather requires activation with either IL-2 or IL-15 (35). In order to understand whether these two cytokines could induce phenotype and functions similar to those of NKp46^{pos} Vδ1 IELs at the level of γδ thymic precursors, we stimulated with both these cytokines γδ thymocytes purified from healthy thymus collected from pediatric patients undergoing cardiac surgical procedures. The activation with either IL-2 or IL-15 induced a statistically significant increase of NKp46, while this was not the case for γδ thymocytes incubated with IL-7 (Figure 5A). Interestingly, the activation with IL-2 induced a preferential expansion of the NKp46^{pos}/Vδ1 T cell subset, as we did not detect any significant proliferation within the Vδ2 cell compartment (Figure 5 B-C). The expansion of Vδ1 thymocytes was mainly associated with an increased de novo expression of NKp46, as we observed very few NKp46^{pos}/Vδ1 cells in freshly isolated thymocytes (data not shown). We also found that IL-2 activation induces a de novo expression of NKp46 on FACS-sorted Vδ1 thymocytes and not on their Vδ2 FACS-sorted counterparts, thus indicating the intrinsic ability of this cytokine to generate NKp46^{pos}/Vδ1 T cell from their thymic Vδ1 precursors without the need of additional cellular interactions (data not shown).

Activation with IL-2 induces on γδ thymocytes also a significant *de novo* expression of NKp44 and NKp30 receptors, although to a less extent compared to that of NKp46. In contrast, we did not detect any induced-expression of NCRs on αβ thymocytes or peripheral γδ T cells following incubation with IL-2 (Figure 5D). Similar results were observed with IL15 (data not shown).

Interestingly, the phenotype of Vδ1 cells expanded from IL-2 activated γδ thymic precursors resembles the one of NKp46^{pos}/Vδ1 IELs freshly purified from human intestine. Indeed, the incubation

with IL-2 (and with IL-15 as well - data not shown) increased on proliferating Vδ1 thymocytes the expression of CD8, CD56 and NKG2D while decreasing the surface levels of CD4. Only NKG2A resulted differently expressed on Vδ1^{pos} cells generated from IL-2 activated thymic precursors compared to freshly purified intestinal NKp46^{pos}/Vδ1 IELs. Indeed, while this latter subset naturally expresses very low levels of this iNKR, the stimulation of thymic precursors with IL-2 induced a remarkably high *de novo* expression of NKG2A on Vδ1^{pos} thymocytes. The IL-2 stimulation also triggered a *de novo* expression on Vδ1^{pos} cells of CCR9, a chemokine-receptor involved in the homing of γδ T lymphocytes to the gut mucosa (Figure 6A) (36). This phenomenon is also functionally relevant as demonstrated by the chemotactic activity of CCR9 on IL-2-activated NKp46^{pos}/Vδ1 thymocytes in response to its CCL25 ligand in a dose-dependent manner (Figure 6B). The acquisition of NKp46 phenotype on γδ thymocytes following incubation with IL-2 is coupled with significantly higher transcription levels of GZMB as well as with an increased degranulation against K562 and human tumor epithelial colorectal Caco2 cell lines (Figures 6C-D).

Taken together, these data indicate that IL-2/IL-15-mediated differentiation of human Vδ1 thymic precursors result in the acquisition of the gut-like phenotype and potent anti-tumor activity by these cells committed to specifically migrate to the gut.

Impact of intestinal microenvironment in the maturation of IL2-activated γδ thymocytes.

The preferential enrichment of NKp46^{pos}/Vδ1 T cells in the intestinal epithelium implicates a tight interaction with intestinal epithelial cells (IECs). Indeed, the survival and the retention of IELs depends on the ligand-activated transcription factor aryl hydrocarbon receptor (AHR) and IL-15 production by neighboring IECs (37). Hence, we incubated γδ thymocytes with IL-2 in the presence or absence of either primary Human Colonic Epithelial cells (HCoEpic) or IL-15. Both these factors had a significant synergistic effect in further increasing the expression of NKp46 on IL-2 activated Vδ1 proliferating thymocytes (Figure 6E). In contrast, we did not observe any change in NKp46 expression on IL-2 activated thymocytes co-cultured with IL-10 or IL-12 or IL-22 or thymic stromal lymphopoietin (TSLP), the soluble factor produced by IECs to induce T cell maturation at this tissue site (38) (data not shown).

We also analyzed the contribution of TGF-β that is overexpressed in CRC with poor prognosis, where this protein plays a key role in the organization of tumor-microenvironment (39). The incubation with TGF-β significantly suppressed the IL-2 induced expression of NKp46 on proliferating γδ thymocytes. Similar inhibitory results were obtained when IL-2-stimulated γδ thymocytes were co-cultured with Caco2 cells (Figure 6E), thus confirming that the intestinal

tumor-microenvironment is endowed with escape mechanisms impairing the cytolytic potential of Vδ1 T cells.

Impact of NKp46^{pos}/Vδ1 IELs on the prognosis and progression of CRC.

We then assessed if the frequency of γδ IELs in the "disease-free/healthy" tissue specimens of patients affected by CRC correlates with tumor progression. To this end, patients included in the analysis were divided into two sub-cohorts either in early (I/II) or late (III/IV) TNM stages of CRC on the basis of the widely-used Tumor-Nodes-Metastasis (TNM) staging system. Patients that required chemotherapy treatment before surgical resection of CRC were excluded from the analyses to avoid any bias on T lymphocytes recurrence. We first observed that the frequencies of total γδ IELs as well as of their Vδ1 and Vδ2 subsets did not change in the portions of healthy colon from CRC patients at different TNM disease stages (Figures 7 A-B). Interestingly, we found that tumor-free gut specimens of CRC patients that progressed toward stages III/IV have a significantly lower frequency of NKp46^{pos}/Vδ1 IELs compared to those at earlier I/II stages. This phenomenon appeared to be specific for NKp46^{pos}/Vδ1 IELs since no changes in the frequencies of NKp46^{pos}/Vδ2 IELs were found between I/II and III/IV CRC stages (Figures 7 C-D).

We then evaluated the ability of the NKp46^{pos}/Vδ1 subset to infiltrate CRC tumor mass. Since this adenocarcinoma originates directly from tumor-transformed IECs and typically disrupt the anatomical organization of gut mucosa in epithelial and lamina propria compartments (Supplemental Figure 1B) (21), we measured the frequency of tumor infiltrating lymphocytes (TILs) on the entire pathologic specimens without distinguishing between IELs and LPLs. We found that the percentages of both total Vδ1 and the NKp46^{pos}/Vδ1 TIL subsets within CRC tumor mass were significantly lower compared to the frequencies of IELs in disease-free/healthy gut tissue specimens (Figures 7 E-F). Since patients affected by IBD are at higher risk of developing CRC (40), we also evaluated the frequency of both Vδ1 cells and NKp46^{pos}/Vδ1 cell subset in patients with ulcerative colitis (UC). Again, the percentages of both these intestinal lymphocyte populations in the UC gut specimens were significantly lower compared to the frequencies of their IEL counterparts in disease-free/healthy gut tissue specimens (Supplemental Figure 7). Taken together, these data suggest that both inflammatory and tumor microenvironments are associated with escape mechanisms inhibiting either the migration or the in-situ expansion of anti-tumor NKp46^{pos}/Vδ1 IELs.

Discussion

NKp46 is one of the three NCRs originally identified as germline encoded proteins specifically expressed on circulating NK cells and playing key roles in cancer-immune-surveillance (41-44). Although NCRs are naturally absent on circulating T cells (17), both NKp46 and NKp44 were previously found to be expressed on human intestinal αβ T cells IELs of patients affected by celiac disease (45). In this context, a major role was played by IL-15, a pro-inflammatory cytokine overexpressed in celiac patients and inducing the expansion of activated NCR^{pos} αβ IELs endowed with potent NK-like and TCR-independent anti-tumor effector-functions (46). However, these cytotoxic NCR^{pos} αβ IELs were highly restricted in their TCR repertoire, thus likely indicating a previous TCR engagement (47). The present study identifies a novel subset of Vδ1 cells constitutively expressing high levels of NKp46 and representing the largest γδ IEL subset in healthy human intestine. $NKp46^{pos}$/Vδ1 IELs are not phylogenetically conserved across species (i.e. mice and humans) and are not present in blood and other human tissue compartments highly enriched in γδ T cells. Hence, they represent a unique population of gut-resident innate-like lymphocytes and a first line of immune-defense against infections and tumors at mucosal interface. This is, to our knowledge, the biggest "natural" (contrasting to induced) (16) NCR^{pos} T cell subset yet identified.

In this study, we also established a methodology able to induce *in vitro* an NCR^{pos} phenotype on pediatric γδ thymocytes upon stimulation with IL-15 or IL-2, which are the two cytokines playing key roles in boosting the γδ T cell cytotoxicity program (35). This is consistent with a previous report showing that both IL-15 and IL-2 (but not IL-7) induces NCR expression and cytotoxicity on T cells (both αβ and γδ) purified from cord blood (48). Further investigation is needed to understand the kinetic and the mechanisms inducing in vivo at the thymus site the expression of NKp46 on Vδ1 thymocytes as well as their ability to migrate to gut epithelium.

We previosly reported an inducible expression of NCRs (with NKp30 being the dominant family member) also on circulating γδ T cells from adult donors, a phenomenon occurring selectively on the Vδ1 T cell subset and requiring both IL-15/IL-2 cell activation and TCR engagement (16). NCR^{pos}/Vδ1 T cells generated from peripheral blood hold great potential for adoptive cell therapy, as they displayed both *in vitro* and *in vivo* (xenograft models) enhanced cytotoxicity against hematological tumors and potent anti-viral activities (49, 50). We show here that the constitutive expression of NKp46 on freshly purified Vδ1 IELs as well as its induced expression on IL-2/IL-15 stimulated Vδ1 thymocyte precursors remarkably increase the cytolytic potential of these innate-like lymphocytes also against solid (epithelial-derived) tumors.

Taken together, these data demonstrate that the presence of NCRs identifies a subset of highly cytotoxic γδ T cells either normally resident in the human gut epithelium or expanded *in vitro* from different sources.

The origin and development of IELs is still the subject of debate. A murine model showed that γδ thymocytes follow maturation waves that sequentially populate different tissues starting with skin at early embryonic age and followed by tongue, reproductive tract and intestine at peri- and post-natal days (51). In the gut there are multiple cellular sources of IL-15 including IECs (37). On the other hand, IL-2 secreted by the neighboring αβ IELs supports the growth of γδ IELs (52). This explains, at least in part, the fact that the intestinal epithelium rather than LP is the preferential "natural" anatomical location for the newly disclosed NKp46^{pos}/γδ IELs. We show here that IL-2 or IL-15 stimulation induces in thymocyte precursors the phenotype and functions of NKp46^{pos}/Vδ1 IELs as well as the expression of CCR9, thus promoting a specific homing of these cells to the IEL compartment (36). In this regard, although IL2/IL15-activated γδ thymocyte precursors share several similarities both in phenotype and functions with freshly purified and gut-resident NKp46^{pos}/Vδ1 IELs, this latter population lacks the expression of NKG2A in contrast to what we observed in IL-2/IL-15 stimulated thymocytes. The different surface distribution of this iNKR is likely associated with the fact that NKp46^{pos}/Vδ1 T cells generated *in vitro* from thymic precursors do not directly interact with IECs naturally expressing high levels of HLA-E. This non-classical MHC-I complex represents the NKG2A natural ligand, whose constitutive high surface level on IECs is a consequence of their chronic stress and antigen challenges occurring at the mucosal interface (53). Hence, the binding of HLA-E with NKG2A on NKp46^{pos}/Vδ1 intestinal IELs might explain its low detectable expression as a mechanism of induced peripheral tolerance under homeostatic conditions and in the presence of alloantigen stimulation. Indeed, NKp46 is involved in the killing of various cancer cells following binding with its natural ligands expressed on cancer cells, a phenomenon also associated with cytoskeletal rearrangement and higher lytic granules polarization to the immune synapse (41, 43, 44, 54, 55). We demonstrate here that the expression of this NCR significantly contributes to the high cytolytic potential of NKp46^{pos}/Vδ1 IELs freshly purified from the gut, since its blocking remarkably reduces this effector-function. Therefore, while NKp46 expression marks an enhanced cytotoxicity among γδ IELs, other receptors such as NKG2A might represent an immune-check point controlling the effector-functions of NKp46^{pos}/Vδ1 intestinal IELs. Additional studies are required to disclose the mechanisms modulating the immune-surveillance thresholds of these newly disclosed subsets of gut resident innate-like lymphocytes. Taken together, these data indicate that the ontogeny and homeostasis of the

NKp46^{pos}/Vδ1 IELs depends both on distinctive features of human Vδ1 thymocytes and gut micro-environmental factors.

The clinical relevance of our newly identified NKp46^{pos}/Vδ1 IELs subset is highlighted by their possible impact in the natural history of CRC. Indeed, our results showed that lower frequencies of NKp46^{pos}/Vδ1 IELs in healthy intestinal tissues surrounding the tumor mass correlate with a higher tumor progression towards metastatic diseases. Interestingly, a recent report showed that the NKp46-mediated production of IFN-γ by NK cells is able to control tumor progression and decreases metastasis *in vivo* via the induced secretion of fibronectin by malignant cells (56). Furthermore, T cells expressing Vδ1 represent the dominant subset among all γδ T cells in CRC patients with an impaired IFN-γ production (21). Our data showed significantly lower frequencies of both CRC intra-tumoral Vδ1 and NKp46^{pos}/Vδ1 T cells compared to those of their counterparts naturally resident in the healthy intraepithelial gut compartment. Incubations of IL-2/IL-15 activated thymocyte precursors with Caco2 cells or TGFβ (overexpressed in CRC) (39) greatly inhibited the expansion of NKp46^{pos}/Vδ1 T cells. Both these *ex vivo* and *in vitro* data suggest that the local tumor-microenvironment might facilitate tumor progression by escaping NKp46^{pos}/Vδ1 IEL cytotoxicity. A recent study reported that the loss of butyrophilin-like (BTLN) molecule BTLN8 coincides with permanent loss of the specific gut-resident BTLN3/8 reactive Vγ4^{pos}/Vδ1 IEL subset upon inflammatory conditions in celiac disease (57). Additional investigations are required to assess if a similar mechanism also contribute to the reduce NKp46^{pos}/Vδ1 T cells in human model of cancer like CRC.

In summary, our identification of a novel gut-resident subset of NKp46^{pos}/Vδ1 IELs endowed with enhanced anti-tumor potential paves the ground for developing novel approaches in the field of immune-therapy. Indeed, both the possibility of generating from thymic precursors *in vitro* NKp46^{pos}/Vδ1 T cells with high tropism for the gut and the "Delta One T cell" protocol (45), which up- regulates NCRs expression on Vδ1 T cells while expanding them to large numbers for adoptive transfer, represent promising and alternative *ad hoc* strategies for CRC treatment.

Methods

Human specimens processing and cell culture

Healthy intestine tissues were collected from the distal area of the pathological tissue (≥ 10 cm) and macroscopically free from any disease. In order to obtain intestinal IELs from healthy intestine tissues, gut mucosa was first dissected from the whole tissue and cut in small pieces, washed in Wash Buffer (WB) prepared with Hank's Balanced salt solution buffer without Ca_2 and Mg_2 (HBSS-/-; Lonza, Verviers, Belgium) supplemented with 1% penicillin/streptomycin/amphotericin (P/S/A; Invitrogen, Paisley, UK), treated with 2 mM of DL-Dithiothreitol (DTT) (Sigma Aldrich, Saint Louis, MO, USA) for 15 min at room temperature (RT), washed again and subsequently treated with 2 mM of Ethylene-diamine-tetra acetic acid (EDTA; Sigma Aldrich) for 30 min at 37°C/5% CO_2. Both cell suspensions were filtered through 100 μm cell strainer (Thermo Fisher Scientific, Waltham, MA, USA) and cells were collected by centrifugation. The remaining tissue was used to isolate lamina propria lymphocytes (LPLs) by enzymatic digestion with 0.75 mg/mL of collagenase II (Sigma Aldrich) for 1 hour at 37°C/5% CO_2. Obtained cells were filtered through 100 μm cell strainer and collected by centrifugation. Finally, both IELs and LPLs were isolated using 30/70% Percoll gradient (Sigma Aldrich). Pathological intestine specimens after they were mechanically minced in small pieces and washed with WB, followed by enzymatic digestion with 1.5 μg/ml of collagenase IV (Life Technologies, Carlsbad, CA), 20μg/ml of hyaluronidase and 50 μg/ml of DNAase (both from Sigma Aldrich) for 2 hours at 37°C/5% CO_2. Obtained cells were isolated by centrifugation and stained for flow cytometry analysis (Supplementary Figures 1A-C).

Human healthy thymus samples were obtained from children undergoing heart surgery for congenital heart diseases according to current clinical practice. Thymic tissue was cleaned from blood vessels and fat tissue and cut in small pieces. Thymocytes were recovered through mechanical smashing and kept in PBS (Corning; New York, NY, USA) with 1% of P/S, to preserve their viability or were frozen in fetal bovine serum (FBS; Lonza) with 10 % of DMSO (Lonza) and stored at -80°C. Thawed thymocytes were cultured in 96 well plate round bottom at a concentration of 10^6 cells /mL in X-VIVO™ 15 serum-free hematopoietic cell medium supplemented with: 5% human AB serum, 1% P/S/A, 1% ultraglutamine, 1% Na pyruvate and 1% of non-essential amino acid solution (NEAA), all purchased from Lonza. Thymocytes cultured *in vitro* were stimulated with human recombinant IL2 (200 U/mL, Miltenyi) or with IL-15, IL-7, IL-10, IL-12, IL-22, TGF-β, thymic stromal lymphopoietin (TSLP), all used at concentration 10 ng/mL and purchased from Peprotech (Rocky Hill, NJ, USA).

Human healthy liver tissues were obtained from patients who underwent hepatectomy for *hepatic metastatic* disease from CRC. Tissue specimens were collected from the distal area of the

pathological tissue (≥ 4cm) and macroscopically free from any disease. Liver tissue dissociation was obtained by enzymatic digestion in gentleMACS™ Dissociator (Miltenyi) with 2 mg/mL of collagenase D (Roche Diagnostic; Indianapolis, IN, USA) for 45 minutes at 37°C/5% CO_2. Cells then were filtered through 100 μm cell strainers, washed in HBSS-/- and lymphocytes were separated using 30/70 % Percoll gradient.

Human healthy skin was obtained from patients who undergo abdominoplasty or mastoplasty surgical procedures. Skin specimens were cut in small pieces and lymphocytes were recuperated by enzymatic digestion with 1.25 U/mL of Dispase II (Roche Diagnostic) initially for 16 hours at 4°C followed by 30 minutes at 37°C. Solution containing epidermal lymphocytes was filtered through 100 μm cell strainers, and cells were washed in HBSS-/- with5mM EDTA. Remaining tissue was further digested with 1 mg/mL collagenase D and 1.25 U/mL of Dispase II 30 minutes at 37°C in order to recover dermis lymphocytes. Cells then were filtered through 100 μm cell strainers, washed in HBSS-/- with 5 mM EDTA and lymphocytes were separated using 30/70 % Percoll gradient.

Human healthy/non-reactive lymph nodes obtained from patients with Whartin's tumor or hyperplasia of salivary glands. Lymph nodes were mechanically smashed in HBSS-/- through 100 μm cell strainers and cells were collected by centrifugation.

Human peripheral blood mononuclear cells (PBMC) were isolated from buffy coats of healthy volunteers (HRH, Rozzano, Italy) using *Lympholyte*® Cell Separation density gradient solution (Cederlane laboratories, Burlington, Canada) according to the manufacturer's instruction.

Primary human colonic epithelial cells (HCoEpic, Cat. No.2950; ScienCell Research Laboratories; Carlsbad, CA, USA) were cultured on poly-L-lysine (Sigma Aldrich) following manufacturer's instructions in the specific colonic epithelial cell medium (CoEpiCM, Cat. No.2951) supplemented with colonic epithelial cell growth supplement (CoEpiCGS, Cat. No.2952) and 1% P/S/A.

Human leukemia cell line K562 (Cat. No.CCL-243; ATCC; Manassas, VA, USA) and colon cancer adenocarcinoma Caco2 (Cat. No.HTB37; ATCC; Manassas, VA, USA), mycoplasma free, were cultured in Iscove's Modified Dulbecco's *medium* (IMDM; Lonza) or Dulbecco's Modified Eagle's medium **(**DMEM; Lonza) respectively, both supplemented with 10% FBS, 1% P/S/A, 1% ultraglutamine. Additional supplements of 1% Na pyruvate and 1% NEAA were added to the Caco2 cell culture medium.

Human SKCO-1 colorectal adenocarcinoma cell line from a metastatic site (ATCC; Cat. No.HTB-39), mycoplasma free, was cultured in Eagle's Minimum Essential medium (EMEM; ATCC) supplemented with 10% FBS and 1% P/S/A.

Mice

Balb-c and *C57BL/6* mice were purchased by Charles River (Wilmington, MA, USA) and maintained under pathogen-free conditions.

Small intestine, colon and spleen specimens were dissected and collected at 4°C in RPMI 1640 (Lonza) medium supplemented with: 10% FBS, 1% P/S/A and 1% ultraglutamine. Cleaned from peyers patches, small intestine and colon tissue were cut in small pieces and treated twice with 1 mM DTT solution (Sigma Aldrich) for 20 min at 37C°/5% CO_2. Cells were then filtered with 70 μm cell strainer and washed with WB. Total lymphocytes were obtained using 30/70% of Percoll gradient (Sigma Aldrich). Spleen was mechanically smashed in a 100 μm cell strainer (Thermo Fisher Scientific), washed with the Wash buffer and filtered in 50 μm cell strainer to obtain single-cell suspension of splenocytes.

Flow cytometry

For multiparametric flow cytometry analysis a standard staining protocol for extracellular markers was used. Briefly, cells were first stained for live/dead discrimination by using Zombie Aqua™ fixable viability kit (BioLegend; San Diego, CA, USA) or 7-Aminoactinomycin D (7-ADD; BD Pharmigen). Subsequently cells were washed with FACS WB (HBSS-/- with 2% of FBS), incubated with antibody (Ab) mix for 20 min in the dark at RT, washed again in and fixed in 1% paraformaldehyde (PFA; Santa Cruz Biotechnology, Dallas, TX, USA). Samples were acquired using LSRFortessa™ cell analyzer system or FACS Canto II (both from BD Bioscience; San Jose, CA, USA). FACS Aria III cell sorter (BD Bioscieces) was used for the specific cell subsets separation and *in vitro* assays, for sorting experiments cells were stained with 7-ADD to discriminate dead cells and the appropriate mix of Abs for 20 min in the dark at RT. The optimal concentration of all Abs used in the study was defined performing a titration experiment. According to the guidelines for an accurate multicolor flow cytometry analysis fluorescence minus one (FMO) controls were used for flow cytometry analysis.

For phenotypic analysis, the following specific anti-human monoclonal antibodies (mAbs; Cat. No/clone) were used. From BioLegend: CD3 (317324/SK7; BV650 and 300306/HIT3a; FITC), CD4 (300534/RPAT4; BV570 or 317438; BV605), CD16 (302025/3G8; AF700), CD69 (310938/FN50; BV605), CD103 (350206/BERACT9; PE), γδ TCR (331208/B1; FITC), NKG2D (320812/ID11; PECy7), NKp46 (331914/9E2; BV421), CCR9 (358906/L053E8; PerCPCy5.5); from BD Biosciences: CD8α (563823/RPAT8; BV780), CD45 (560566/H130; AF700 and 557833/2D1; APCCy7), CD56 (562289/B159; PE-CF594), CD69 (555533/FN50; APC); NKp30 (563383/P3015; BV711); from Miltenyi Biotec (Bergish Gladbach, Germany): CD45 (130096609/5B1; APCVio770), KIRs

(130103937/REA293; APCVio770 and 130095285/DX27; PerCPCy5.5), Vδ1 (130120440/REA173; PE and 130100542; PEVio770), NKG2A (130098812/REA111; APC), from eBioscience: CD8β (25527342/5IDI8BEE; PECy7), from Beckman Coulter (Brea, CA,USA) Vδ2 (IM1464/IMMU-389; FITC) and NKp44 (PNA66903/Z231; PECy5); from R&D system (Minneapolis, MN, USA) NKG2C (FAB138C/134591; PerCP).

Mouse γδ T lymphocytes were stained with live/dead discriminating marker 7-ADD and with the specific anti-mouse mix of mAbs: CD3 (555274/17A2; FITC), NKp46 (561169/29A1.4; AF700) (both from BD Pharmigen) and γδ TCR (17571182/eBioGL3; APC) (eBioscience).

Cell cytotoxic activity was assessed by CD107a flow cytometry-based assay. Freshly isolated effector IELs or thymocytes were plated in 96 well plate at a concentration 10^6 cells/mL in the presence or not of target cells K562 or Caco2 at a ratio of E:T=1:1 in X-VIVO™ 15 complete medium and 8 μg/mL of PE-conjugated anti-CD107a Ab (555801/H4A3; BD Biosciences). After 4 hours of incubation at 37°C/5% CO_2 cells were collected, washed in HBSS-/- and stained for extracellular markers as described above. PBMC obtained from healthy donors pre-stimulated 1 hour with PMA (0.5 μg/mL) and Ionomycin (0.1 μg/mL) (both from Sigma Aldrich) were used as the control of the degranulation assay. For masking experiments, the specific anti-hNKp46 IgM blocking mAb (KL247) was kindly provided by Prof. Silvia Parolini, University of Brescia, Brescia, Italy (58).

Intracellular IFN-γ, TNF-α and GZMB accumulation was measured by flow cytometry. Freshly isolated IELs were plated in 96 well plate round bottom at a concentration of 10^6 cells /mL with or without target cells K562 at a ratio of E:T = 1:1 and in the presence of 1μg/mL of Golgi Plug, protein transport inhibitor (BD Biosciences). As a protein transport inhibitor (containing Brefeldin A), Golgi Plug, was able to trap the amounts of newly synthesize (i.e. increased intracellulare levels) Granzyme B and IFN-γ at intracellular site in response to activation stimuli. After 4 hours at 37°C/5% CO_2 IELs were collected, washed with HBSS-/- and extracellular staining as described above was performed. Subsequently intracellular staining was done using Cytofix/Cytoperm™ and Perm/Wash™ kits (BD Biosciences) according to the manufacturer's instructions and using specific anti-human Abs (BD Biosciences) for for TNF-α (559321/Mab11; PE), IFN-γ (564039/B27; BV711) and GZMB (560212/GB11; AF647).

For chemotaxis experiments, viable $CD45^{pos}$/$CD3^{pos}$/γδ TCR^{pos}/$NKp46^{pos}$ IL-2 activated human thymocytes were sorted and plated in X-VIVO™ 15 complete medium in the basket of the trans-well with 8.0 μm large pore (Corning). Human recombinant CCL25 (BioLegend) was added to the bottom of the trans-wells at different concentration 0, 25 and 50 ng/mL and left 6 hours at 37°C/5% CO_2. After this time cells were collected and counted by LSRFortessa™ flow cytometry for quantification.

High-throughput analysis of TRG and TRD repertoires

CDR3 regions of either the γ-chain (TRG) or δ-chain (TRD) were amplified from flow cytometry-sorted NKp46^{pos} and NKp46^{neg} Vδ1 IELs via a previously described mRNA-based multiplex PCR amplification method (59). PCR amplicons were indexed with the Illumina Nextera Index Kit, purified with Agencourt AMPure beads, equally pooled with 96-samples and sequenced at the Illumina MiSeq platform (paired-end, 500 cycles, high-output) as recommended by Illumina guidelines, while 20% PhIX was used as a spike-in control. The obtained fastq files of read1 were annotated with MiXCR software (60) using default parameters and further analyzed with the R package TcR (**PMID: 26017500**) and VDJtools (61, 62). For TRD repertoires only Vδ1^{pos} sequences were processed after MiXCR annotation. Treemaps were generated with the R package treemap. The deposited bio-project number is PRJNA558198

qPCR

Total RNA of sorted γδ T NKp46^{pos} and NKp46^{neg} IELs/thymocytes was extracted using RNasy micro-plus columns with RNase-free DNase treatment and RNA carrier (Qiagen Valencia, CA, USA) following the manufacturer's instructions. Extracted RNA was used to generate cDNA templates for qPCR using High-Capacity cDNA Reverse Transcription Kit with random primers and RNase inhibitor (Applied Biosystem, Foster City, CA, USA). 100 ng of total cDNA were pre-amplified for the specific gene expression using TaqMan®mRNA gene assays and TaqMan® PreAmp Master Mix (both from Applied Biosystem). QPCR reactions were performed by Real Time AB7900 (Applied Biosystem) with TaqMan® Universal PCR Master Mix and the specific TaqMan®mRNA gene assays (Applied Biosystem): NCR1 (HS00183683), IL10 (HS00961622), IL17A (HS00174383), TGFβ (HS00998133), IL22 (HS01574154), IFNγ (HS00989291), GZMB (HS01554355), XCL1 (HS00751481) and housekeeping S18 (HS01026310) and GAPDH (HS02758991). PCR-based detection of mycoplasmal DNA was performed using BioMix™ (Bioline, London, UK) and GPO-1 (5'-ACTCCTACGGGAGGCAGCAGT-3') and MGSO (5' -TGCACCATCTGTCACTCTGTTAACCTC-3') primers from IDT (Coralville, IA, USA).

Immunohistochemistry and Immunofluorescence

Formalin-fixed paraffin-embedded liver specimens, previously sectioned with a microtome HM310 Microm (GMI, MN, USA) at 2-4 μm thickness and mounted onto charged glass slides Superfrost^{+} (Thermo Fisher Scientific), were stained with H&E using a standard protocol. Briefly, after two changes of xylenes, rehydration in an ethanol/water gradient (100%, 90%, 70%), followed

by washing in water, slides were stained with in Mayer's Hematoxylin solution (Dako, CA; USA) for 18 min, differentiated under running tap water for 10 min, then stained with 1% aqueous solution of Y Eosin (Dako) for 8 min, followed by three washes with 100% ethanol, and three washed with xylenes. Lastly H&E stained slides were mounted with Eukitt (Sigma Aldrich) and dried prior to imaging by Microscope BX51 (Olympus, Tokyo, Japan).

Freshly isolated tissues were fixed with 4% paraformaldehyde for 2 hours, washed and incubated overnight in 30% sucrose. Tissues were then embedded in OCT, frozen in a bath of isopentane cooled on dry ice, and cut in 8 μm-thick sections. Human NKp46 staining was then performed using polyclonal goat anti-human NKp46 (Cat. No.AF1850; R&D Systems; used 20 μg/mL), polyclonal rabbit anti-human CD3 (No.A0452; Dako, CA; USA; diluted 1:50) and mouse monoclonal anti-human TCR-PAN γδ (COIM1349/IMMU510) (10 μg/mL) then followed by the following secondary antibodies raised in donkey (Invitrogen): anti-rabbit Alexa488, anti-mouse Alexa594, and anti-goat Alexa647, all used at concentration of 1:1000. Nuclei were counterstained with DAPI (Invitrogen) at concentration of 1:50000. After staining, slides were dried, mounted with Prolong Gold (Invitrogen) and examined under Zeiss LSM 510 confocal microscope (Zeiss, Germany). Image processing was performed with Zeiss LSM and Adobe Photoshop software

Statistics

Statistical analyses were performed using GraphPad Prism version 7. For the comparison of two matched groups of samples (specified in the legend) Wilcoxon *t* test was applied or non-paired Mann-Whitney *t* test was applied. Experiments with more than two groups were analyzed by Kruskal-Wallis with Dunn's post-hoc multiple comparisons test. When specified, Pearson's data correlation and R-Squared analyses were used. The data are depicted as vertical bars corresponding to mean value ±estimated standard error (SEM) with scatter dots or as box and whisker plots with the median value displayed inside the box and the maximum and minimum values displayed with whiskers. Some graphs are represented as scattered plots of paired observations. P values > 0.05 were considered not statistically significant (ns). Statistically significant P values were represented with GraphPad (GP) style and summarized with following number of asterisks (*): *$P \leq 0.05$; **$P \leq 0.01$; ***$P \leq 0.001$; ****$P \leq 0.0001$. Flow cytometry data were analyzed by FlowJo software version 9.4 and 9.6 (FlowJo LLC; Ashland, OR, USA). Flow cytometry data analysis based on t-SNE algorithm were performed using FlowJo 9.6 software.

Study approval

Patient recruitment and samples collection have been performed according to the Declaration of Helsinki. The collection of human samples for research purposes was ethically approved by the Institutional review Board (IRB) of Humanitas Research Hospital (HRH) for blood and gut specimens either free of diseases of affected by CRC or Inflammatory Bowel Diseases (IBDs) of patients undergoing surgical gut resection and for healthy skin of patients undergoing plastic surgical procedures (approval 2012/1021), for healthy lymph nodes of patients undergoing the removal of benign head-neck tumors (approval 2010/700), for healthy liver specimens of patients undergoing resection of CRC metastasis (approval 168/18). We also received IRB approval from the University Hospital of Palermo (UNIPA) for the collection of gut specimens affected by CRC of patients undergoing surgical gut resection (approval 13/2013) and from the IRB of TIGET/San Raffaele Institute for specimens of healthy thymus from pediatric patients undergoing cardiac surgery (approval TIGET07, TCTO-044). All participants or parents with the custody of the child undergoing cardiac surgery were informed about the aims of this research program and signed a detailed informed consent.

Animal experiments adhered to the requirements of the European Commission Directive 86/609/EEC and to the Italian legislation (Decreto Legislativo 116; 27 January 1992). Experiments were approved by the Animal Care and Use Committee from Italian Ministry of Health (approval 158/2011).

Author Contributions

J.M., F.O., E.B., A.R., B.S.S. and D.M. designed and performed experiments; A.V., M.B., I.B., E.L.P., S.M., F.D., S.V., S.D., S.D.B., M.M.C., M.S., G. Cu., G. Co., E.M., M.K. and A.S. provided biological specimens, reagents and experimental protocols; F.S.C. provided assistance with flow cytometry and cell sorting; P.S. and M.R. provided pathologic examination of tissue specimens; I.P., S.R. and B.L. performed TCR repertoire sequencing and analysis; J.M., F.O. and D.M. designed the study, analyzed data and wrote the manuscript; D.M. directed the study.

Acknowledgments

The authors thank the patients for their generosity and participation in this study and the nurses of the Colon and Rectal Surgery Unit (Humanitas Clinical and Research Center). We thank Matteo Cimino, Matteo Donadon and Guido Torzilli from Humanitas Clinical and Research Center and Humanitas University for providing specimens of human healthy liver, Genni Enza Marcovecchio from San Raffaele Scientific Institute for providing specimens of healthy human thymus. We thank Kelly Hudspeth, Elena Pontarini and Manuela Lo Porto from Humanitas Clinical and Research Center for their help in the implementation of experimental protocols and Stefano Mantero from Consiglio Nazionale delle Ricerche for his support in immunochemistry. We thank also Prof. Silvia Parolini from University of Brescia, Brescia, Italy for anti-NKp46 blocking mAb.

This work was supported by Associazione Italiana per la Ricerca sul Cancro (IG 14687 to D.M), by the Italian Ministry of Health (Bando Giovani Ricercatori GR2011023477381 to K.H. and GR-2013-02356522 to A.R.) and intramural research and clinical funding programs of Humanitas Research Hospital (to D.M.) and by Fondazione Telethon (SR-Tiget F3 core grant to MB) and National Program of CNR Aging Project (to A.V).

Competing Interests

B.S.-S. is a co-founder and shareholder of Lymphact – Lymphocyte Activation Technologies S.A. The remaining authors declared no competing financial interests.

References

1. *Mowat, A.M., and Agace, W.W. 2014. Regional specialization within the intestinal immune system. Nat Rev Immunol 14:667-685.*
2. *Gopalakrishnan, V., Spencer, C.N., Nezi, L., Reuben, A., Andrews, M.C., Karpinets, T.V., Prieto, P.A., Vicente, D., Hoffman, K., Wei, S.C., et al. 2018. Gut microbiome modulates response to anti-PD-1 immunotherapy in melanoma patients. Science 359:97-103.*
3. *Deusch, K., Luling, F., Reich, K., Classen, M., Wagner, H., and Pfeffer, K. 1991. A major fraction of human intraepithelial lymphocytes simultaneously expresses the gamma/delta T cell receptor, the CD8 accessory molecule and preferentially uses the V delta 1 gene segment. Eur J Immunol 21:1053-1059.*
4. *Chien, Y.H., Meyer, C., and Bonneville, M. 2014. gammadelta T cells: first line of defense and beyond. Annu Rev Immunol 32:121-155.*
5. *Nielsen, M.M., Witherden, D.A., and Havran, W.L. 2017. gammadelta T cells in homeostasis and host defence of epithelial barrier tissues. Nat Rev Immunol 17:733-745.*
6. *Roberts, S.J., Smith, A.L., West, A.B., Wen, L., Findly, R.C., Owen, M.J., and Hayday, A.C. 1996. T-cell alpha beta + and gamma delta + deficient mice display abnormal but distinct phenotypes toward a natural, widespread infection of the intestinal epithelium. Proc Natl Acad Sci U S A 93:11774-11779.*
7. *Fujihashi, K., Dohi, T., Kweon, M.N., McGhee, J.R., Koga, T., Cooper, M.D., Tonegawa, S., and Kiyono, H. 1999. gammadelta T cells regulate mucosally induced tolerance in a dose-dependent fashion. Int Immunol 11:1907-1916.*
8. *Vantourout, P., and Hayday, A. 2013. Six-of-the-best: unique contributions of gamma delta T cells to immunology. Nature Reviews Immunology 13:88-100.*
9. *Bottino, C., Tambussi, G., Ferrini, S., Ciccone, E., Varese, P., Mingari, M.C., Moretta, L., and Moretta, A. 1988. Two subsets of human T lymphocytes expressing gamma/delta antigen receptor are identifiable by monoclonal antibodies directed to two distinct molecular forms of the receptor. J Exp Med 168:491-505.*
10. *Scotet, E., Martinez, L.O., Grant, E., Barbaras, R., Jeno, P., Guiraud, M., Monsarrat, B., Saulquin, X., Maillet, S., Esteve, J.P., et al. 2005. Tumor recognition following V gamma 9V delta 2 T cell receptor interactions with a surface F1-ATPase-related structure and apolipoprotein A-I. Immunity 22:71-80.*
11. *Tanaka, Y., Morita, C.T., Nieves, E., Brenner, M.B., and Bloom, B.R. 1995. Natural and synthetic non-peptide antigens recognized by human gamma delta T cells. Nature 375:155-158.*
12. *Gober, H.J., Kistowska, M., Angman, L., Jeno, P., Mori, L., and De Libero, G. 2003. Human T cell receptor gamma delta cells recognize endogenous mevalonate metabolites in tumor cells. Journal of Experimental Medicine 197:163-168.*
13. *Zou, C., Zhao, P., Xiao, Z., Han, X., Fu, F., and Fu, L. 2017. gammadelta T cells in cancer immunotherapy. Oncotarget 8:8900-8909.*
14. *Silva-Santos, B., Serre, K., and Norell, H. 2015. gammadelta T cells in cancer. Nat Rev Immunol 15:683-691.*
15. *Correia, D.V., Lopes, A., and Silva-Santos, B. 2013. Tumor cell recognition by gammadelta T lymphocytes: T-cell receptor vs. NK-cell receptors. Oncoimmunology 2:e22892.*
16. *Correia, D.V., Fogli, M., Hudspeth, K., da Silva, M.G., Mavilio, D., and Silva-Santos, B. 2011. Differentiation of human peripheral blood Vdelta1+ T cells expressing the natural cytotoxicity receptor NKp30 for recognition of lymphoid leukemia cells. Blood 118:992-1001.*
17. *Hudspeth, K., Silva-Santos, B., and Mavilio, D. 2013. Natural cytotoxicity receptors: broader expression patterns and functions in innate and adaptive immune cells. Frontiers in Immunology 4.*
18. *Wu, D., Wu, P., Qiu, F.M., Wei, Q.C., and Huang, J. 2017. Human gamma delta T-cell subsets and their involvement in tumor immunity. Cellular & Molecular Immunology 14:245-253.*
19. *Pang, D.J., Neves, J.F., Sumaria, N., and Pennington, D.J. 2012. Understanding the complexity of gammadelta T-cell subsets in mouse and human. Immunology 136:283-290.*
20. *Gentles, A.J., Newman, A.M., Liu, C.L., Bratman, S.V., Feng, W., Kim, D., Nair, V.S., Xu, Y., Khuong, A., Hoang, C.D., et al. 2015. The prognostic landscape of genes and infiltrating immune cells across human cancers. Nat Med 21:938-945.*

21. *Meraviglia, S., Lo Presti, E., Tosolini, M., La Mendola, C., Orlando, V., Todaro, M., Catalano, V., Stassi, G., Cicero, G., Vieni, S., et al. 2017. Distinctive features of tumor-infiltrating gammadelta T lymphocytes in human colorectal cancer. Oncoimmunology 6:e1347742.*
22. *Gibbons, D.L., and Spencer, J. 2011. Mouse and human intestinal immunity: same ballpark, different players; different rules, same score. Mucosal Immunol 4:148-157.*
23. *Sathaliyawala, T., Kubota, M., Yudanin, N., Turner, D., Camp, P., Thome, J.J., Bickham, K.L., Lerner, H., Goldstein, M., Sykes, M., et al. 2013. Distribution and compartmentalization of human circulating and tissue-resident memory T cell subsets. Immunity 38:187-197.*
24. *Cepek, K.L., Shaw, S.K., Parker, C.M., Russell, G.J., Morrow, J.S., Rimm, D.L., and Brenner, M.B. 1994. Adhesion between epithelial cells and T lymphocytes mediated by E-cadherin and the alpha E beta 7 integrin. Nature 372:190-193.*
25. *Hayday, A., Theodoridis, E., Ramsburg, E., and Shires, J. 2001. Intraepithelial lymphocytes: exploring the Third Way in immunology. Nat Immunol 2:997-1003.*
26. *Kadivar, M., Petersson, J., Svensson, L., and Marsal, J. 2016. CD8 alpha beta(+) gamma delta T Cells: A Novel T Cell Subset with a Potential Role in Inflammatory Bowel Disease. Journal of Immunology 197:4584-4592.*
27. *Hunter, S., Willcox, C.R., Davey, M.S., Kasatskaya, S.A., Jeffery, H.C., Chudakov, D.M., Oo, Y.H., and Willcox, B.E. 2018. Human liver infiltrating gammadelta T cells are composed of clonally expanded circulating and tissue-resident populations. J Hepatol 69:654-665.*
28. *Hudspeth, K., Donadon, M., Cimino, M., Pontarini, E., Tentorio, P., Preti, M., Hong, M., Bertoletti, A., Bicciato, S., Invernizzi, P., et al. 2016. Human liver-resident CD56(bright)/CD16(neg) NK cells are retained within hepatic sinusoids via the engagement of CCR5 and CXCR6 pathways. J Autoimmun 66:40-50.*
29. *Tomasello, E., Yessaad, N., Gregoire, E., Hudspeth, K., Luci, C., Mavilio, D., Hardwigsen, J., and Vivier, E. 2012. Mapping of NKp46(+) Cells in Healthy Human Lymphoid and Non-Lymphoid Tissues. Front Immunol 3:344.*
30. *Di Lorenzo, B., Ravens, S., and Silva-Santos, B. 2019. High-throughput analysis of the human thymic Vdelta1(+) T cell receptor repertoire. Sci Data 6:115.*
31. *Bamias, G., Arseneau, K.O., and Cominelli, F. 2014. Cytokines and mucosal immunity. Curr Opin Gastroenterol 30:547-552.*
32. *Boismenu, R., Feng, L., Xia, Y.Y., Chang, J.C., and Havran, W.L. 1996. Chemokine expression by intraepithelial gamma delta T cells. Implications for the recruitment of inflammatory cells to damaged epithelia. J Immunol 157:985-992.*
33. *Gomes, A.Q., Correia, D.V., Grosso, A.R., Lanca, T., Ferreira, C., Lacerda, J.F., Barata, J.T., da Silva, M.G., and Silva-Santos, B. 2010. Identification of a panel of ten cell surface protein antigens associated with immunotargeting of leukemias and lymphomas by peripheral blood gamma delta T cells. Haematologica-the Hematology Journal 95:1397-1404.*
34. *Van de Walle, I., Waegemans, E., De Medts, J., De Smet, G., De Smedt, M., Snauwaert, S., Vandekerckhove, B., Kerre, T., Leclercq, G., Plum, J., et al. 2013. Specific Notch receptor-ligand interactions control human TCR-alpha beta/gamma delta development by inducing differential Notch signal strength. Journal of Experimental Medicine 210:683-697.*
35. *Ribot, J.C., Ribeiro, S.T., Correia, D.V., Sousa, A.E., and Silva-Santos, B. 2014. Human gammadelta thymocytes are functionally immature and differentiate into cytotoxic type 1 effector T cells upon IL-2/IL-15 signaling. J Immunol 192:2237-2243.*
36. *Kabelitz, D., and Wesch, D. 2003. Features and functions of gamma delta T lymphocytes: Focus on chemokines and their receptors. Critical Reviews in Immunology 23:339-370.*
37. *Qiu, Y., Wang, W., Xiao, W., and Yang, H. 2015. Role of the intestinal cytokine microenvironment in shaping the intraepithelial lymphocyte repertoire. J Leukoc Biol 97:849-857.*
38. *Ziegler, S.F., and Liu, Y.J. 2006. Thymic stromal lymphopoietin in normal and pathogenic T cell development and function. Nature Immunology 7:709-714.*
39. *Tauriello, D.V.F., and Batlle, E. 2016. Targeting the Microenvironment in Advanced Colorectal Cancer. Trends Cancer 2:495-504.*

40. *Janakiram, N.B., and Rao, C.V. 2014. The role of inflammation in colon cancer. Adv Exp Med Biol 816:25-52.*
41. *Glasner, A., Ghadially, H., Gur, C., Stanietsky, N., Tsukerman, P., Enk, J., and Mandelboim, O. 2012. Recognition and prevention of tumor metastasis by the NK receptor NKp46/NCR1. J Immunol 188:2509-2515.*
42. *Moretta, A., Bottino, C., Mingari, M.C., Biassoni, R., and Moretta, L. 2002. What is a natural killer cell? Nat Immunol 3:6-8.*
43. *Lakshmikanth, T., Burke, S., Ali, T.H., Kimpfler, S., Ursini, F., Ruggeri, L., Capanni, M., Umansky, V., Paschen, A., Sucker, A., et al. 2009. NCRs and DNAM-1 mediate NK cell recognition and lysis of human and mouse melanoma cell lines in vitro and in vivo. J Clin Invest 119:1251-1263.*
44. *Halfteck, G.G., Elboim, M., Gur, C., Achdout, H., Ghadially, H., and Mandelboim, O. 2009. Enhanced in vivo growth of lymphoma tumors in the absence of the NK-activating receptor NKp46/NCR1. J Immunol 182:2221-2230.*
45. *Meresse, B., Curran, S.A., Ciszewski, C., Orbelyan, G., Setty, M., Bhagat, G., Lee, L., Tretiakova, M., Semrad, C., Kistner, E., et al. 2006. Reprogramming of CTLs into natural killer-like cells in celiac disease. Journal of Experimental Medicine 203:1343-1355.*
46. *Meresse, B., Chen, Z., Ciszewski, C., Tretiakova, M., Bhagat, G., Krausz, T.N., Raulet, D.H., Lanier, L.L., Groh, V., Spies, T., et al. 2004. Coordinated induction by IL15 of a TCR-independent NKG2D signaling pathway converts CTL into lymphokine-activated killer cells in celiac disease. Immunity 21:357-366.*
47. *Meresse, B., Curran, S.A., Ciszewski, C., Orbelyan, G., Setty, M., Bhagat, G., Lee, L., Tretiakova, M., Semrad, C., Kistner, E., et al. 2006. Reprogramming of CTLs into natural killer-like cells in celiac disease. J Exp Med 203:1343-1355.*
48. *Tang, Q., Grzywacz, B., Wang, H., Kataria, N., Cao, Q., Wagner, J.E., Blazar, B.R., Miller, J.S., and Verneris, M.R. 2008. Umbilical cord blood T cells express multiple natural cytotoxicity receptors after IL-15 stimulation, but only NKp30 is functional. J Immunol 181:4507-4515.*
49. *Almeida, A.R., Correia, D.V., Fernandes-Platzgummer, A., da Silva, C.L., da Silva, M.G., Anjos, D.R., and Silva-Santos, B. 2016. Delta One T Cells for Immunotherapy of Chronic Lymphocytic Leukemia: Clinical-Grade Expansion/Differentiation and Preclinical Proof of Concept. Clinical Cancer Research 22:5795-5804.*
50. *Hudspeth, K., Fogli, M., Correia, D.V., Mikulak, J., Roberto, A., Della Bella, S., Silva-Santos, B., and Mavilio, D. 2012. Engagement of NKp30 on Vdelta1 T cells induces the production of CCL3, CCL4, and CCL5 and suppresses HIV-1 replication. Blood 119:4013-4016.*
51. *Allison, J.P., Asarnow, D.M., Bonyhadi, M., Carbone, A., Havran, W.L., Nandi, D., and Noble, J. 1991. Gamma delta T cells in murine epithelia: origin, repertoire, and function. Adv Exp Med Biol 292:63-69.*
52. *Chu, C.L., Chen, S.S., Wu, T.S., Kuo, S.C., and Liao, N.S. 1999. Differential effects of IL-2 and IL-15 on the death and survival of activated TCR gamma delta+ intestinal intraepithelial lymphocytes. J Immunol 162:1896-1903.*
53. *Perera, L., Shao, L., Patel, A., Evans, K., Meresse, B., Blumberg, R., Geraghty, D., Groh, V., Spies, T., Jabri, B., et al. 2007. Expression of nonclassical class I molecules by intestinal epithelial cells. Inflamm Bowel Dis 13:298-307.*
54. *Bloushtain, N., Qimron, U., Bar-Ilan, A., Hershkovitz, O., Gazit, R., Fima, E., Korc, M., Vlodavsky, I., Bovin, N.V., and Porgador, A. 2004. Membrane-associated heparan sulfate proteoglycans are involved in the recognition of cellular targets by NKp30 and NKp46. Journal of Immunology 173:2392-2401.*
55. *Hadad, U., Thauland, T.J., Martinez, O.M., Butte, M.J., Porgador, A., and Krams, S.M. 2015. NKp46 clusters at the immune synapse and regulates NK cell polarization. Frontiers in Immunology 6.*
56. *Glasner, A., Levi, A., Enk, J., Isaacson, B., Viukov, S., Orlanski, S., Scope, A., Neuman, T., Enk, C.D., Hanna, J.H., et al. 2018. NKp46 Receptor-Mediated Interferon-gamma Production by Natural Killer Cells Increases Fibronectin 1 to Alter Tumor Architecture and Control Metastasis. Immunity 48:107-119 e104.*
57. *Mayassi, T., Ladell, K., Gudjonson, H., McLaren, J.E., Shaw, D.G., Tran, M.T., Rokicka, J.J., Lawrence, I., Grenier, J.C., van Unen, V., et al. 2019. Chronic Inflammation Permanently Reshapes Tissue-Resident Immunity in Celiac Disease. Cell 176:967-981 e919.*

58. *Pende, D., Parolini, S., Pessino, A., Sivori, S., Augugliaro, R., Morelli, L., Marcenaro, E., Accame, L., Malaspina, A., Biassoni, R., et al. 1999. Identification and molecular characterization of NKp30, a novel triggering receptor involved in natural cytotoxicity mediated by human natural killer cells. J Exp Med 190:1505-1516.*
59. *Ravens, S., Schultze-Florey, C., Raha, S., Sandrock, I., Drenker, M., Oberdorfer, L., Reinhardt, A., Ravens, I., Beck, M., Geffers, R., et al. 2017. Human gammadelta T cells are quickly reconstituted after stem-cell transplantation and show adaptive clonal expansion in response to viral infection. Nat Immunol 18:393-401.*
60. *Bolotin, D.A., Poslavsky, S., Mitrophanov, I., Shugay, M., Mamedov, I.Z., Putintseva, E.V., and Chudakov, D.M. 2015. MiXCR: software for comprehensive adaptive immunity profiling. Nat Methods 12:380-381.*
61. *Nazarov, V.I., Pogorelyy, M.V., Komech, E.A., Zvyagin, I.V., Bolotin, D.A., Shugay, M., Chudakov, D.M., Lebedev, Y.B., and Mamedov, I.Z. 2015. tcR: an R package for T cell receptor repertoire advanced data analysis. BMC Bioinformatics 16:175.*
62. *Shugay, M., Bagaev, D.V., Turchaninova, M.A., Bolotin, D.A., Britanova, O.V., Putintseva, E.V., Pogorelyy, M.V., Nazarov, V.I., Zvyagin, I.V., Kirgizova, V.I., et al. 2015. VDJtools: Unifying Post-analysis of T Cell Receptor Repertoires. PLoS Comput Biol 11:e1004503.*

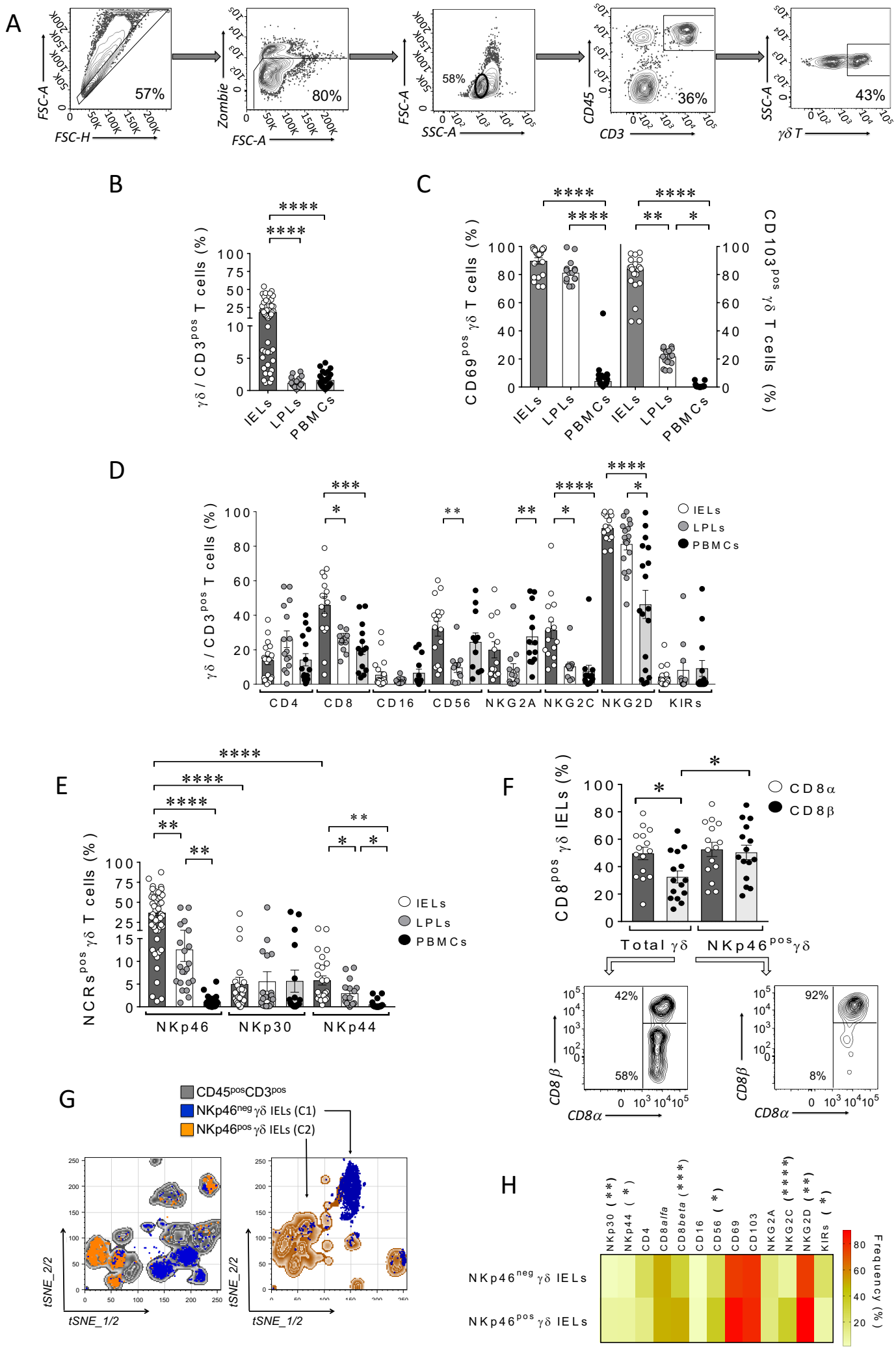

Mikulak J. et al. Figure 1

Figure 1.

Identification of a novel subset of NKp46^{pos} intraepithelial Vδ1 T lymphocytes highly enriched in human healthy intestine.

(A) Representative example of flow cytometry dot plots showing the gating strategy used to identify viable CD45^{pos}/CD3^{pos} γδ T lymphocyte both in intraepithelial (IEL) and lamina propria (LPL) compartments from specimens of human healthy colon. **(B)** Summary statistical graph showing within the CD45^{pos}/CD3^{pos} lymphocytes the percentages of γδ IELs (N=54 in white circles), γδ LPLs (N=20 in gray circles) from human healthy colon specimens and γδ peripheral blood mononuclear cells (PBMCs) (N=26 in black circles) of healthy donors. **(C)** Summary statistical graph showing the expression (%) of CD69 (left) and CD103 (right) on γδ IELs (N=20 in white circles), γδ LPLs (N=15 in grey circles) from specimens of human healthy colon and on γδ T cell from PBMCs (N=20 in black circles) of healthy donors. **(D)** Summary statistical graph showing the expression (%) of CD4, CD8, CD16, CD56, NKG2A, NKG2C, NKG2D and Killer Immunoglobulin-like Receptors (KIRs) on γδ IELs (N ≥13 in white circles), γδ LPLs (N ≥10 in gray circles) from specimens of human healthy colon and on γδ T cells from PBMCs of healthy donors (N ≥13 in black circles). **(E)** Summary statistical graph showing the expression (%) of NKp46, NKp30 and NKp44 on γδ IELs (N ≥25 in white circles), γδ LPLs (N ≥16 in gray circles) from specimens of human healthy colon and on γδ T cells from PBMCs from healthy donors (N ≥25 in black circles). **(F)** Summary statistical analysis (upper graph) showing the expression (%) of CD8α (white circles) and CD8β (black circles) chains within the CD8 receptor of matched CD8^{pos} γδ IELs and CD8^{pos}/NKp46^{pos} γδ IELs from specimens of human healthy colon (N=15). White arrows indicate representative flow cytometry dot plots showing co-expression of CD8α and CD8β chains respectively in CD8^{pos} total γδ T (left) or NKp46^{pos}/γδ T (right) IELs. **(G)** t-SNE graphs from a representative specimen of human healthy colon showing the clustering of NKp46^{neg} (C1 in blue) and NKp46^{pos} (C2 in orange) γδ IELs within CD45^{pos} /CD3^{pos} lymphocytes (gray; left panel) or in γδ T IELs (right panel). **(H)** Heat-map graph showing the degree of expression of several surface markers on matched NKp46^{neg} and NKp46^{pos} γδ IELs clusters defined as C1 and C2 in panel G (N=7).

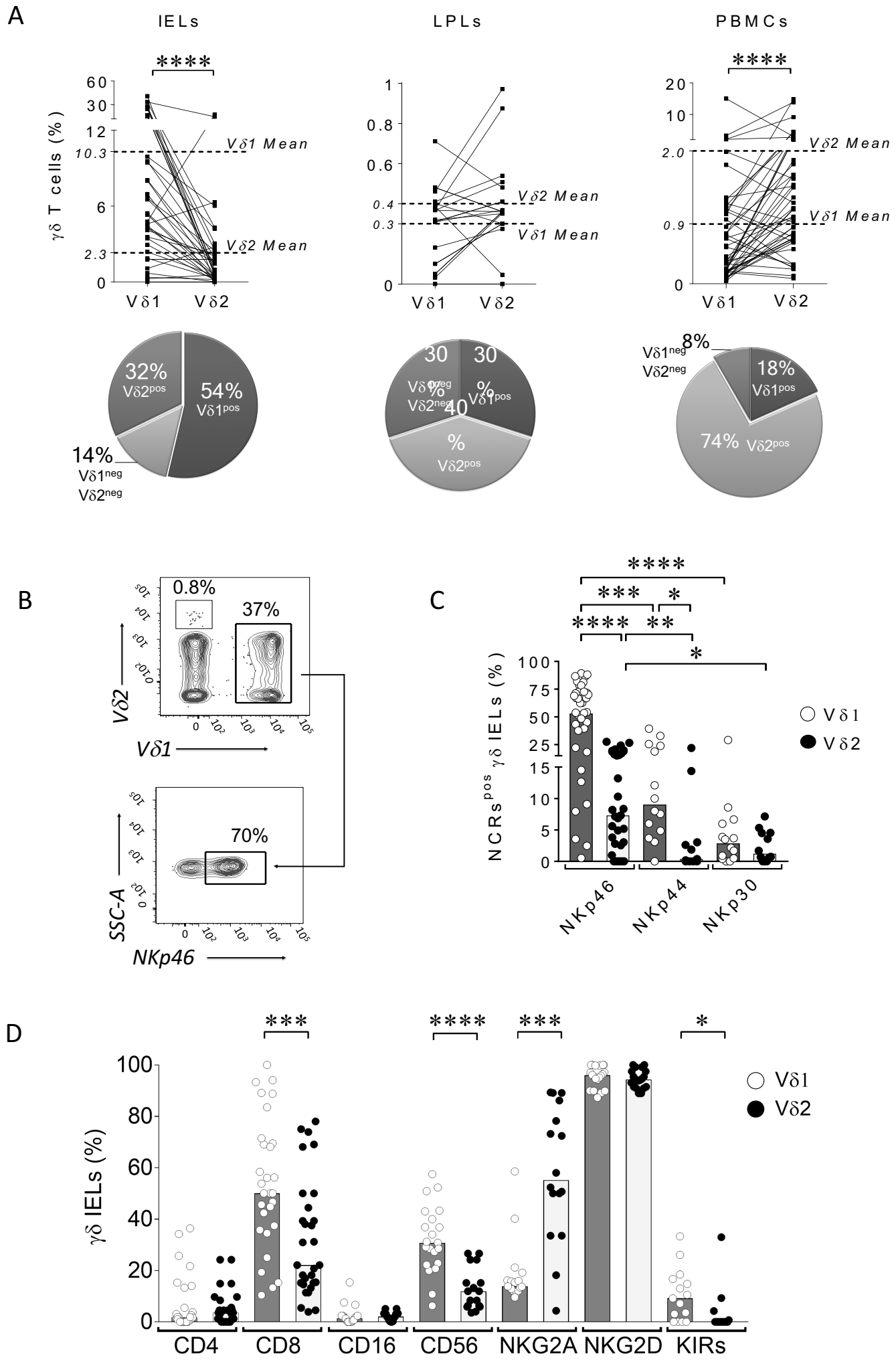

Mikulak J. et al. Figure 2

Figure 2.

NKp46^{pos} γδ IELs are Vδ1 restricted and express a cytotoxic phenotype.

(A) Summary statistical graphs (upper line) showing within the entire CD45^{pos}/CD3^{pos} lymphocyte population the percentages of Vδ1 or Vδ2 IEL (N=37) and LPL (N ≥22) subsets from specimens of human healthy colon and from PBMCs (N=49) of healthy donors. Data are represented as scattered plots of paired observations. Pie charts (lower line) showing the percentages of Vδ1^{pos}, Vδ2^{pos} and Vδ1^{neg}/Vδ2^{neg} subsets within total γδ T cells of matched samples (N=10) of IELs and LPLs from specimens of human healthy colon and PBMCs of healthy donors. **(B)** Representative examples (out of 38) of contour plots showing the percentages of Vδ1^{pos} and Vδ2^{pos} T cell subset (upper panel) and of NKp46^{pos}/Vδ1 T cells (lower panel) within total purified γδ IELs from a specimen of human healthy colon. **(C)** Summary statistical graph showing the frequencies of Vδ1 (white circles) and Vδ2 (black circles) IELs (N ≥20) from specimens of human healthy colon expressing NKp46, NKp44 and NKp30. **(D)** Summary statistical graph showing the frequencies of Vδ1 (white circles) and Vδ2 (black circles) IELs (N ≥16) from specimens of human healthy colon expressing CD4, CD8, CD16, CD56, NKG2A, NKG2D and Killer Immunoglobulin-like Receptors (KIRs).

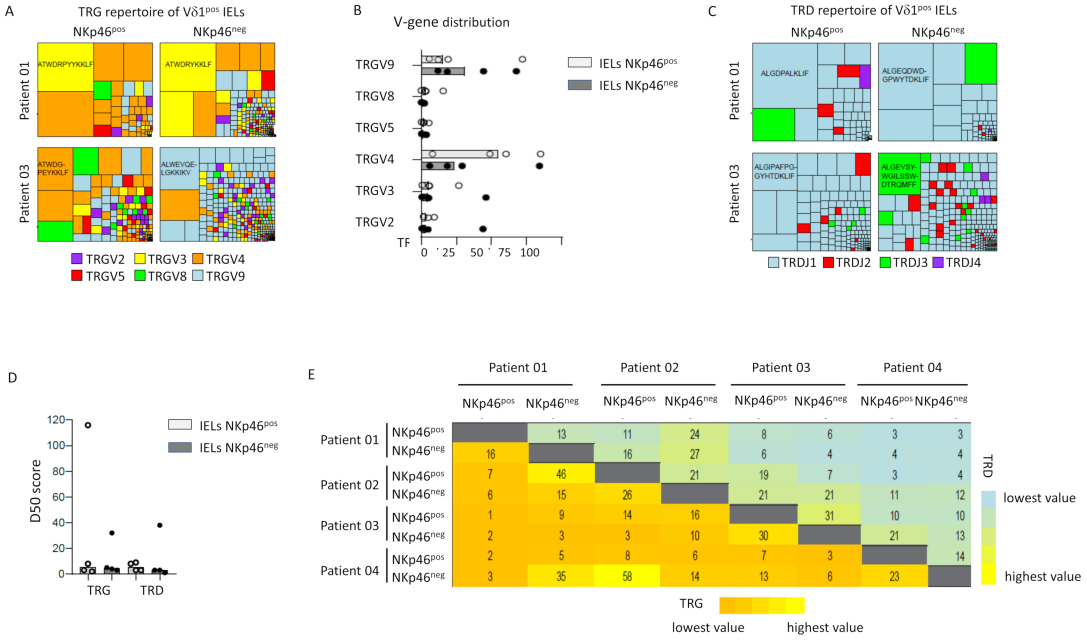

Mikulak J. et al. Figure 3

Figure 3.

TCR repertoires of NKp46^{pos} and NKp46^{neg} γδ IELs.

(A) Treemap graphs showing the distribution of TRG clones within NKp46^{pos} and NKp46^{neg} γδ IELs from two representative patients (out of 4). Squares represent individual clones and are proportional to the abundance of the given clone within the TCR repertoire. Color codes indicate V-chain usage. CDR3 sequences of the most expanded clones are given. **(B)** Dot plot graph showing the quantification of V-chains for TRG repertoires. Each dot represents one patient. **(C)** Treemap graphs showing the distribution of Vδ1^{pos} TRD clones within NKp46^{pos} and NKp46^{neg} IELs of two patients. Each square indicates one clone within the given TRD repertoires. J-elements are color coded and CDR3 sequences of the most expanded clones are indicated. **(D)** Dot plot graph showing the TRG and TRD diversity that is determined by the D50 score (number of clones within 50% of the given TCR repertoire). Each dot represents one patient. **(E)** Heatmap graph displaying the number of shared TRG (lower part, orange - yellow) and TRD (upper part, blue - yellow) clones between patients' samples.

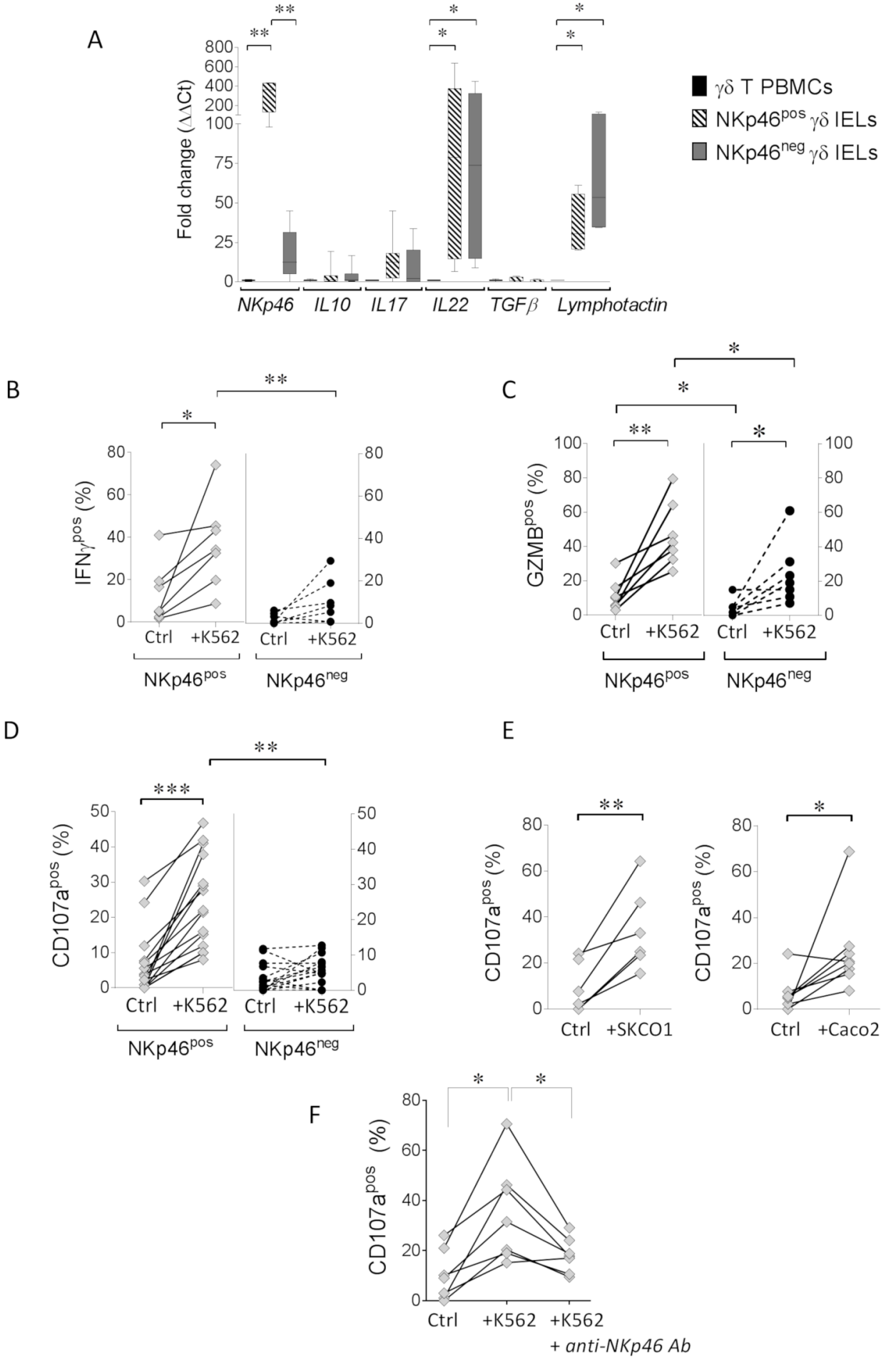

Mikulak J. et al. Figure 4

Figure 4.

Effector-functions of NKp46^{pos} γδ IELs.

(A) Summary statistical graphs showing the transcript levels of NKp46, IL-10, IL-17, IL-22, TGF-β, and lymphotactin/XCL1 and in FACS-sorted NKp46^{pos} and NKp46^{neg} γδ IELs from specimens of human healthy colon (N=6) and in FACS-sorted γδ T cell from PBMCs of healthy donors (N=6). Results are presented as fold changes ($2^{-\Delta\Delta CT}$) of target gene relative to PBMC samples and normalized to housekeeping genes GAPDH and S18. **(B-D)** Summary statistical graphs showing the intracellular levels of IFN-γ **(B)**, Granzyme B (GMZB) **(C)** and surface expression of CD107a **(D)** by NKp46^{pos} and NKp46^{neg} γδ IELs from specimens of human healthy colon either in the absence (Ctrl) or in the presence of K562 cell lines. **(E)** Summary statistical graphs showing the surface expression of CD107a by NKp46^{pos} γδ IELs from healthy colon either alone or in co-culture with tumor target cells SKCO1 (left) and Caco2 (right). **(F)** Summary statistical graph showing the surface expression of CD107a by NKp46^{pos} γδ IELs from healthy colon after co-culture with K562 either in the absence or presence of a blocking anti-NKp46 IgM mAb (N=7).

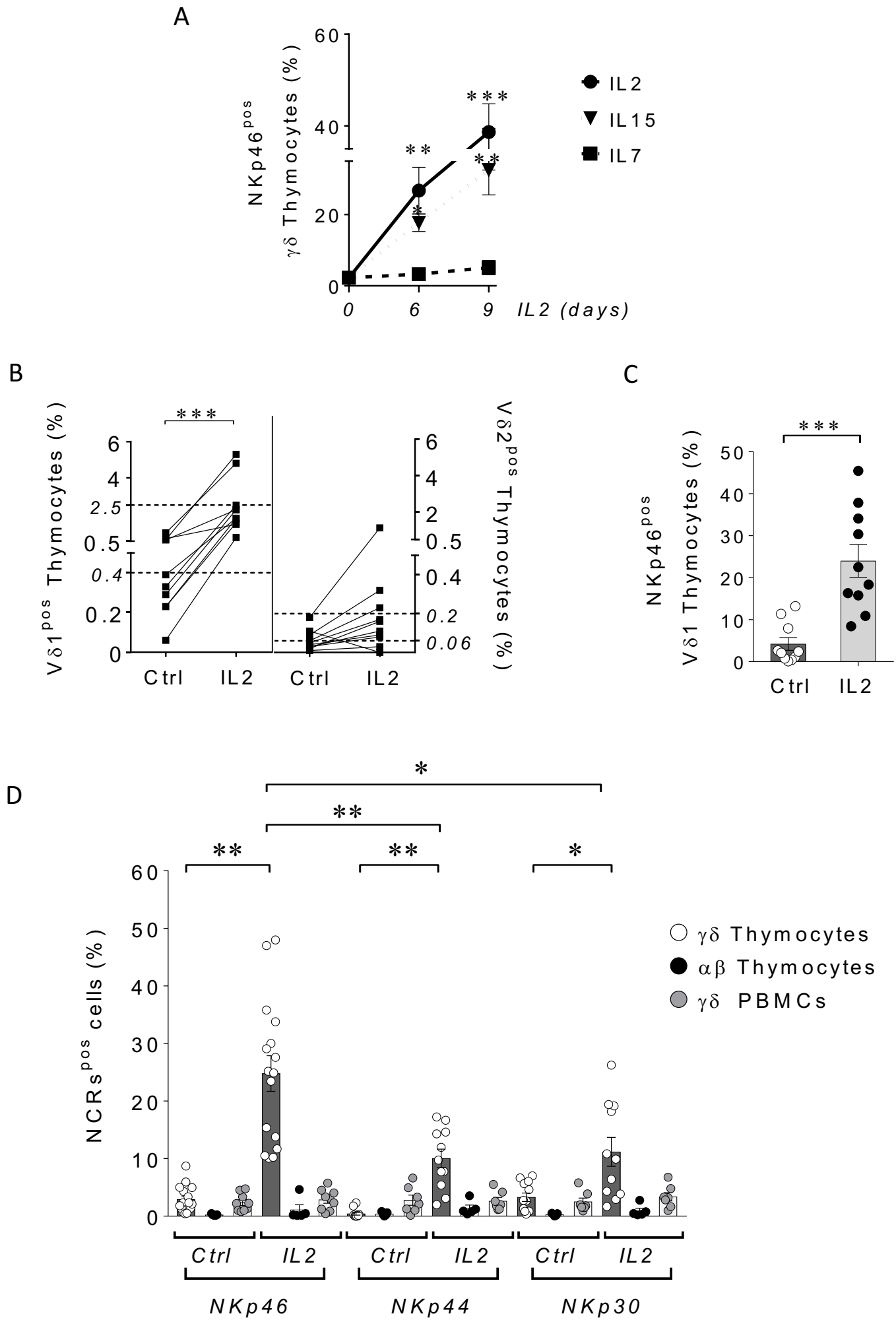

Mikulak J. et al. Figure 5

Figure 5.

NKp46^{pos}/Vδ1 T cell expansion following activation of thymocyte precursors with IL-2 or IL-15.

(A) Summary statistical graphs showing the time course expression of NKp46 in γδ thymocyte precursors (N ≥5) cultured with IL-2 (200 U/mL) or IL-15 (10 ng/mL) or IL-7 (10 ng/mL). **(B)** Summary statistical graphs showing the frequencies of Vδ1 (left graph) and Vδ2 (right graph) thymocytes cultured either in absence (Ctrl) or presence of IL-2 for 6 days (N=10). Data are represented as scattered plots of paired observations. **(C)** Summary statistical graphs showing the frequency of NKp46 expression on Vδ1 thymocytes cultured either in the absence (Ctrl) or in the presence of IL-2 for 6 days (N=10). **(D)** Summary statistical graphs showing NCR expression in γδ and αβ thymocytes as well as in γδ T cells from PBMCs of healthy donor cultured either in absence (Ctrl) or in the presence of IL2 for 6 days (N ≥5).

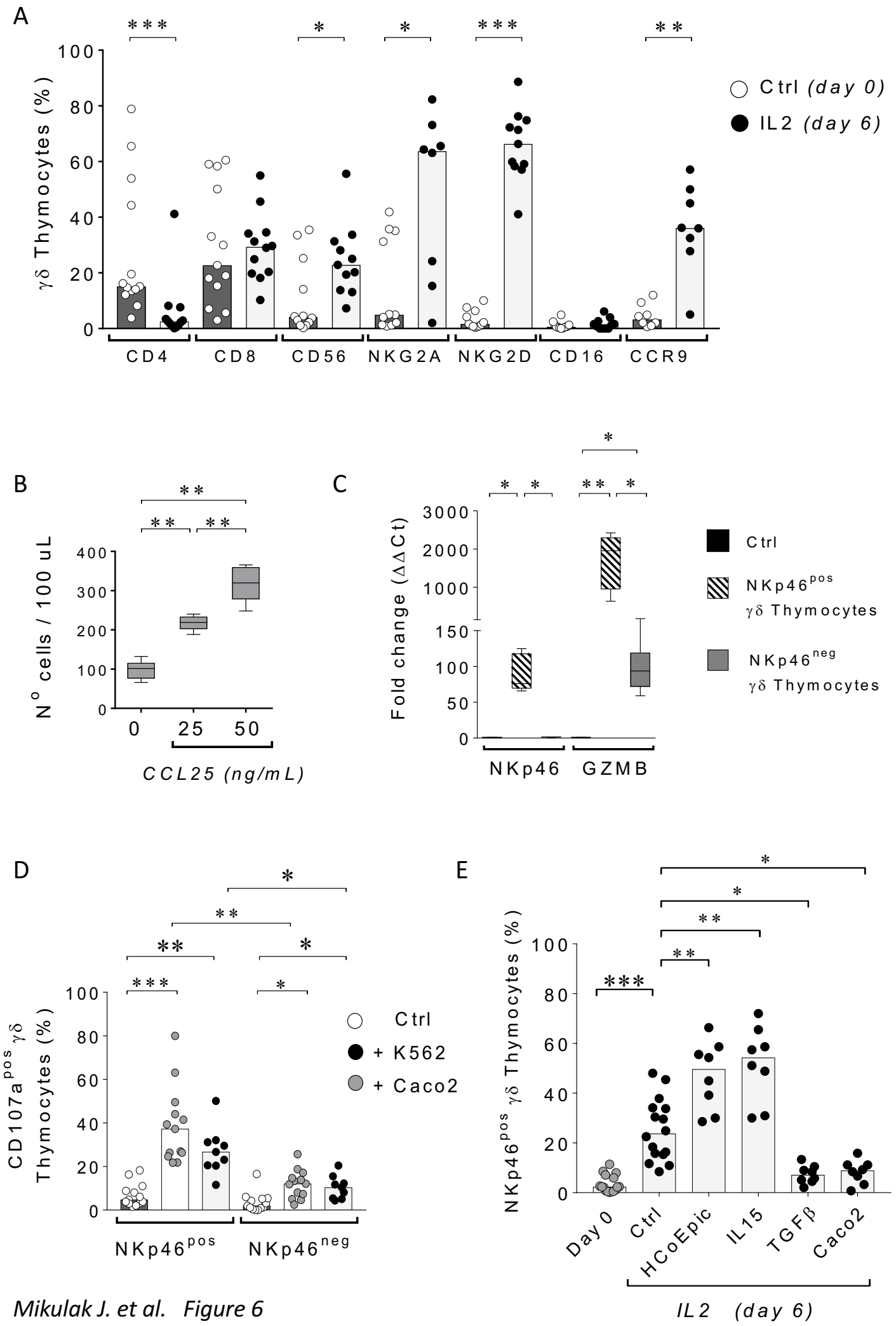

Mikulak J. et al. Figure 6

Figure 6.

Phenotype and functions of human of NKp46^{pos} γδ thymocyte precursors following activations with physiologic and pathologic stimuli.

(A) Summary statistical graphs showing the expression of CD4, CD8, CD56, NKG2A, NKG2D, CD16 and CCR9 on γδ thymocyte precursors (N ≥ 8) cultured either in the absence (Ctrl) or presence of IL-2. **(B)** Summary statistical graphs showing the CCL25 dose-dependent chemotaxis of FACS-sorted CCR9^{pos}/NKp46^{pos} Vδ1 T cells generated from thymocyte precursors cultured with IL-2 for 6 days (N=8). **(C)** Summary statistical graphs showing the transcripts levels of GZMB and NKp46 transcripts on freshly FACS-sorted thymocytes (Ctrl) and on NKp46^{pos} and NKp46^{neg} Vδ1 T cells generated from thymocyte precursors cultured with IL-2 for 6 days (N=6). Results are represented as the fold change ($2^{-\Delta\Delta CT}$) of target gene relative to a Ctrl samples and normalized to housekeeping genes GAPDH and S18. **(D)** Summary statistical graphs showing the expression of CD107a on NKp46^{pos} and NKp46^{neg} Vδ1 T cells generated from thymocyte precursors cultured with IL-2 for 6 days either in the absence (Ctrl) or in the presence of K562 or Caco2 human tumor target cells (N ≥ 9). **(E)** Summary statistical graphs showing the NKp46 expression on freshly purified thymocytes (Day 0) and on γδ thymocytes cultured with IL-2 for 6 days either in the absence (Ctrl) or in the presence of primary human colonic epithelial cells (HCoEpic) or IL-15 or TGF-β or Caco2 cell line (N ≥ 8).

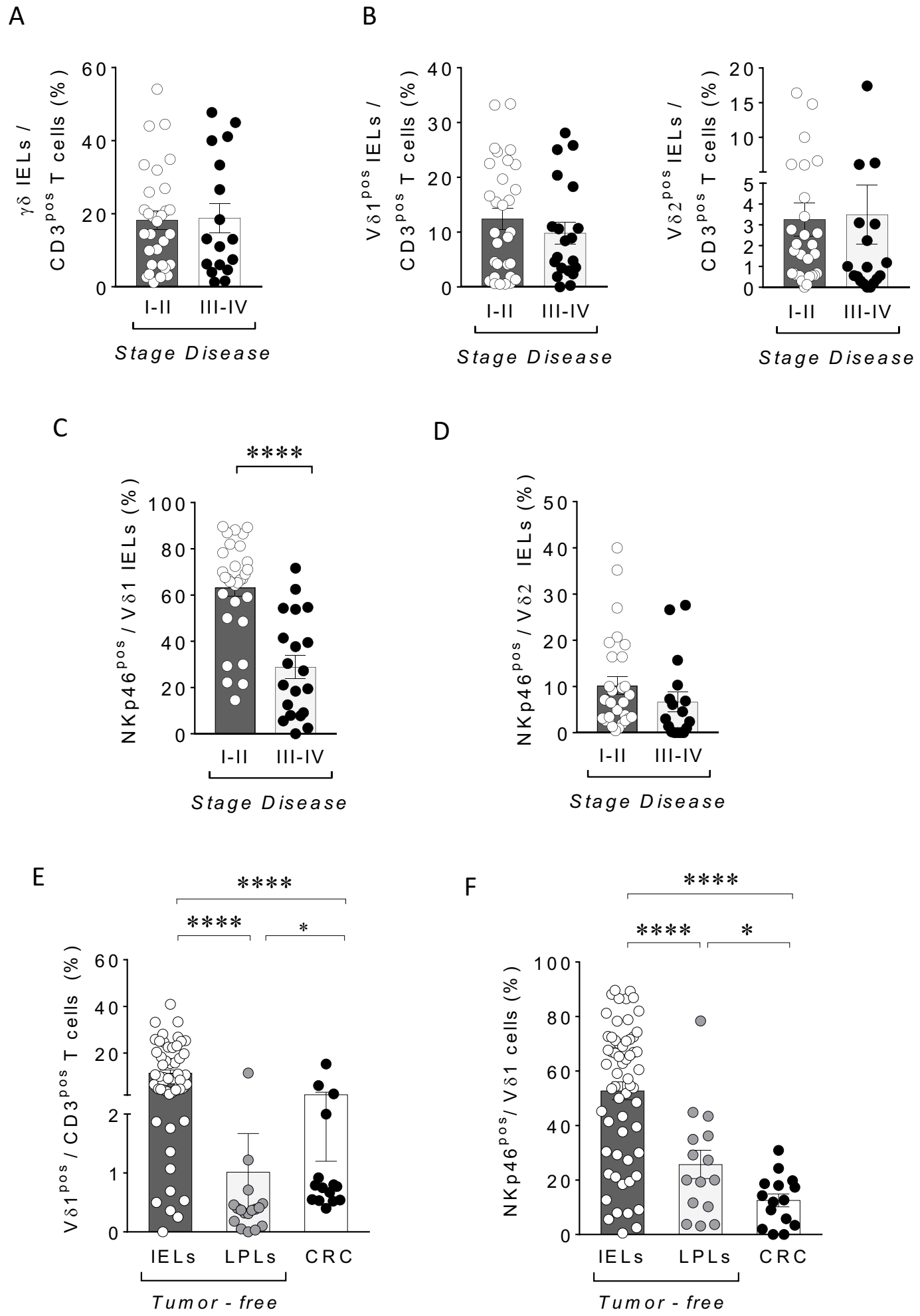

Mikulak J. et al. Figure 7

Figure 7.

Clinical relevance of the NKp46^{pos}/Vδ1 subset in the pathogenesis of CRC.

(A-D) Summary statistical graphs showing the frequencies of total γδ **(A),** Vδ1 and Vδ2 **(B**), NKp46^{pos}/Vδ1 **(C**) and NKp46^{pos}/Vδ2 **(D)** IEL subsets in healthy intestinal specimens from CRC patients in early (I-II) and late (III-IV) disease stages (N ≥17). **(E-F)** Summary statistical graphs showing the frequencies of total Vδ1 cells **(E)** and of the NKp46^{pos}/Vδ1 T cell subset **(F)** in both IELs and LPLs compartments of healthy/disease-free intestine compared to those of infiltrating gut specimens of colon rectal cancer (CRC) (N ≥ 15).